UNIVERSIDAD DE CHILE
FACULTAD DE CIENCIAS FÍSICAS Y MATEMÁTICAS
DEPARTAMENTO DE INGENIERÍA ELÉCTRICA

RESILIENT PLANNING OF THE NEW ZEALAND POWER SYSTEM IN LIGHT OF HYDROGEN INTEGRATION THROUGH THE REMIX-NZ ENERGY OPTIMIZATION FRAMEWORK

TESIS PARA OPTAR AL GRADO DE MAGÍSTER EN CIENCIAS DE LA INGENIERÍA, MENCIÓN ELÉCTRICA

MEMORIA PARA OPTAR AL TÍTULO DE INGENIERA CIVIL ELÉCTRICA

MELISSA ANAÍS ALÉ MARTÍNEZ

PROFESOR GUÍA:
RODRIGO MORENO VIEYRA

MIEMBROS DE LA COMISIÓN:
JANNIK HAAS
ÁNGELA FLORES QUIROZ

SANTIAGO DE CHILE
2024

RESUMEN DE LA TESIS PARA OPTAR
AL GRADO DE MAGÍSTER EN CIENCIAS
DE LA INGENIERÍA, MENCIÓN ELÉCTRICA Y
MEMORIA PARA OPTAR AL TÍTULO DE
INGENIERA CIVIL ELÉCTRICA
POR: MELISSA ANAÍS ALÉ MARTÍNEZ
FECHA: 2024
PROF. GUÍA: RODRIGO MORENO VIEYRA

PLANIFICACIÓN RESILIENTE DEL SISTEMA ELÉCTRICO DE NUEVA ZELANDA CONSIDERANDO LA INTEGRACIÓN DE HIDRÓGENO MEDIANTE EL FRAMEWORK REMIX-NZ

Numerosos estudios han destacado la importancia de la planificación resiliente para las transiciones energéticas sostenibles durante fenómenos meteorológicos extremos. Es crucial evaluar la flexibilidad técnica y el posible estrés de integrar nuevos vectores energéticos, como el hidrógeno, debido al aumento de la demanda de electricidad. Este estudio utiliza un marco de resiliencia que se basa en datos históricos y proyecciones de futuro para evaluar los estados de daño y vulnerabilidad de los componentes del sistema eléctrico mediante curvas de fragilidad y curvas de recuperación. A continuación, la información se utiliza como entrada para la herramienta de optimización del sistemas energéticos REMix-NZ para calcular las métricas de resiliencia. El estudio de caso comparó la resiliencia de distintas distribuciones espciales de recursos de hidrógeno en el sistema eléctrico de Nueva Zelanda en 2050 durante eventos sísmicos. Los escenarios de distirbucioón considerados fueron distribuido, intermedio y concentrado. Los resultados mostraron que la topología de demanda de hidrógeno distribuida presentaba una mayor resiliencia ante los eventos, con una menor carga e hidrógeno no servido en comparación con la producción centralizada a gran escala. Además, el coste total del sistema resultó ser el más bajo. Basándose en estos resultados, se recomienda el establecimiento de centros de energía de hidrógeno distirbudios en todo el país. El trabajo de este estudio sobre planificación resiliente en REMIx-NZ puede utilizarse para analizar otros riesgos naturales para crear un sistema energético con capacidad de respuesta ante cualquier contingencia.

RESUMEN DE LA TESIS PARA OPTAR
AL GRADO DE MAGÍSTER EN CIENCIAS
DE LA INGENIERÍA, MENCIÓN ELÉCTRICA Y
MEMORIA PARA OPTAR AL TÍTULO DE
INGENIERA CIVIL ELÉCTRICA
POR: MELISSA ANAÍS ALÉ MARTÍNEZ
FECHA: 2024
PROF. GUÍA: RODRIGO MORENO VIEYRA

RESILIENT PLANNING OF THE NEW ZEALAND POWER SYSTEM IN LIGHT OF HYDROGEN INTEGRATION THROUGH THE REMIX-NZ ENERGY OPTIMIZATION FRAMEWORK

Numerous studies have emphasized the importance of resilience planning for sustainable energy transitions during extreme weather events. It is crucial to evaluate the technical flexibility and potential stress of integrating new energy carriers, such as hydrogen, due to the increased electricity demand. This study utilizes a resilience framework that draws on historical data and forward-looking projections to evaluate the power system components' hazard and vulnerability states through fragility curves and recovery-based restoration curves. The information is then used as input for the REMix-NZ energy system optimization tool to calculate the resiliency metrics. The case study employed a comparative approach to examine the impact of different spatial distributions of hydrogen resources on the resilience of the New Zealand electricity system in 2050 during seismic events. The distribution scenarios considered were concentrated, intermediate and distributed. Results showed that the distributed hydrogen demand scenario exhibited enhanced resilience to seismic events, with reduced load and hydrogen not served compared to large-scale concentrated production. Moreover, the total system cost was found to be the lowest. Therefore, it is advised that the distributed spatial distribution of hydrogen energy hubs be established nationwide. This study's work on resilient planning in REMIx-NZ can be used to analyze other natural hazards and create a responsive energy system for any contingencies.

Para Matilda,
y por un mundo mejor para ella.

Agradecimientos

A mis padres, Sandra y Víctor, por entregarme amor y apoyo incondicional, permitiéndome superar todos los desafíos que me he propuesto en la vida. A mi hermana Danissa, por siempre escucharme y darme sus consejos, más alguna incoherente broma interna. A mi hermano Víctor y a mi sobrina Matilda, por existir. A mis perritos Simio y Pupa, por acompañarme en todas las noches que pasé en vela. Soy muy afortunada de que sean mi familia, los quiero.

A Vicente, el amor de mi vida, por celebrar cada uno de mis triunfos como si fueran propios, por alentarme durante los períodos de dudas e inseguridades, por recorrer el mundo para volver a verme, por concederme el honor y la inestimable felicidad de ser mi compañero de vida, entre tantas cosas más. Te admiro demasiado y no puedo esperar a seguir aprendiendo de ti y contigo. Te amo con cada latido de mi corazón y en cada suspiro de mi existencia.

A Valentina, mi mejor amiga, por una amistad que nunca ha buscado nada más que hacernos compañía en este mundo que a veces nos parece tan aterrador. Gracias por siempre estar al otro lado de la línea y por tus increíbles tallitas.

A mis amigas Victoria, Débora, Ignacia y Constanza, por las múltiples rumbas de celebración y las infinitas juntas de apoyo emocional. A mis amigos Byron y Marcelo, por responder a todos mis llamados de emergencia. Muchas gracias por estar siempre, pandilla.

A Consuelo, Camila y Paola, por su amistad incodicional desde los años mozos de bachillerato. Gracias por tantas risas e insólitas historias compartidas.

A las ingeniosas, Cote, Majo y Barbi, que aparecieron en mi camino más vale tarde que nunca, pero a quienes agradezco infinitamente haber encontrado. Muchas gracias por tantas risas, copuchas y choques de copas que espero se vuelvan tradición.

A Rafaella, mi mejor amiga kiwi, por todas las risas y llantos compartidos, por ser tan auténtica y por todos los paseos a mi lugar favorito del mundo, el Arts Centre de Christchurch.

A Jannik Haas por ser un gran mentor y por invitarme a Nueva Zelanda a vivir una experiencia que me cambiaría la vida para siempre. Gracias por haberme hecho sentir en casa incluso estando lejos y por siempre apoyarme para ser mejor.

A mi profesor guía, Rodrigo Moreno, por su sabiduría y apoyo durante este proceso, y a la profesora Ángela Flores, por formar parte de mi comisión.

Por último, a todas las y los que me acompañaron en algún momento de este largo camino.

Table of Content

Tables Index

Figures Index

Chapter 1

Introduction

1.1. Motivation

The energy transition represents an essential and pressing global challenge. This need stems from the imperative to mitigate climate change, ensure energy security, and meet the increasing demand for clean, sustainable energy. Renewable resources and new energy carriers, such as hydrogen, are vital for achieving a low-carbon economy [1]. In light of the pressing urgency of the transition, it is crucial to implement resilient planning of national electricity systems. This introduces several technical challenges, including the intermittency of supply and demand management. However, it allows for significant reductions in carbon footprints, thereby building a more sustainable and adaptable energy infrastructure to meet future energy needs.

The effective management of the energy transition necessitates the development and utilization of advanced planning tools. These tools facilitate strategic decision-making for the expansion and operation of energy systems by integrating various technologies. They also consider the complex interdependencies between electricity, heat, transportation, and industry sectors [2]. Power system expansion and operation optimization tools, such as REMix (Renewable Energy Mix for a Sustainable Energy Supply) [3], are particularly useful in this regard. Such tools facilitate strategic decisions to align renewable energy supply with demand, plan long-term investments, and develop robust, resilient infrastructures [4].

The rapid and constant evolution of energy systems in terms of the integration of new efficient technologies justifies the need to plan and operate resilient power systems. These are grids capable of anticipating, preparing, absorbing, recovering, and adapting their operation and infrastructures to the occurrence of High-Impact, Low-Probability (HILP) events [5]. This ensures the reliability, stability, and adaptability of the power supply.

Reliable planning is of paramount importance for the extended grid to be sufficient and secure. This necessitates that the generation and transmission infrastructure must be capable of meeting demand at all times. Furthermore, they should also withstand disturbances and contingencies, maintaining system integrity by returning to its normal state after credible and known events [6].

In contrast, resilient planning is required for less frequent but more disruptive events. These may include natural disasters such as hurricanes, tornadoes, earthquakes, tsunamis, or volcanic activity. Furthermore, events associated with extreme weather conditions, such as heat waves, wildfires, floods, landslides, or strong wind gusts, must also be taken into consideration [7].

Earthquakes, being a phenomenon that is inherently unpredictable, can have a significant impact on energy systems. The objective of resilient planning against such threats is to prepare networks to respond effectively to seismic events. This entails both the physical resilience of the infrastructure and the system's capacity to maintain generation and demand [7], [8]. The role of fragility and restoration curves in this process is of crucial importance. These curves describe the probability of electrical components sustaining damage based on the intensity of the threat and the time required for recovery, given the extent of the damage [9]. The data thus obtained facilitates the prediction of the behaviour of the system during an earthquake, thereby enabling the calculation of infrastructure and energy "state of health" metrics. These metrics quantify the system's resilience in the event of such disruptive occurrences.

The integration of a resilience study into an energy system planning tool, which considers hydrogen as a strategic component, is a crucial yet under-researched area. As an energy carrier, hydrogen can enhance the flexibility and robustness of an energy system due to its versatility and storage capacity [10].

Given the imminent inclusion of hydrogen as an energy vector in future power systems, it is of the utmost importance to gain insight into how different spatial distributions of hydrogen resources (distributed, intermediate, and concentrated) respond to disruptive events such as earthquakes. This understanding is of paramount importance for the optimization of infrastructure planning and emergency response strategies.

In this context, the use of a power system optimization tool such as REMix becomes crucial. The software facilitates the optimization and analysis of various disconnection scenarios based on parameters describing the earthquake's impact on electrical components. This allows for the development of effective and resilient planning strategies.

This study focuses on the New Zealand electricity system, which makes it an ideal case study for earthquake-resilient planning for several reasons. Firstly, New Zealand boasts a diverse electricity portfolio, primarily composed of renewable energies [11]. The self-sufficient, isolated system is currently dominated by hydroelectric power. Moreover, the country's considerable spatial and natural resources (including high solar radiation and wind speeds) facilitate the expansion of a diversified system, a factor of interest in terms of seismic risk expansion.

Secondly, New Zealand is situated in the Pacific Ring of Fire, an area that corresponds to one of the most seismically active regions of the Pacific Ocean [12]. In addition, the country has a historical precedent of earthquakes, including the Christchurch earthquake in 2011, which resulted in 75 % of the city being without electricity [13]. This event has provided valuable insights into the impact of seismic events on energy systems.

Finally, New Zealand has a significant commitment to reducing emissions and transitioning to a more sustainable energy system, as evidenced by the Emissions Reduction Plan (2022) [14], which presents strategies to introduce technologies such as solar and wind energy, hydrogen, and batteries. These energy carriers require resilient planning, especially the latter two, which are key in energy storage and grid flexibility. Consequently, this study on the integration of hydrogen in earthquake resilience planning offers a future perspective that is applicable to other regions in similar contexts.

In order to enhance the resilience of New Zealand's national power system against natural disasters, it is essential to assess the impact of integrating a novel energy carrier in line with the national objectives outlined in the Hydrogen Roadmap [15] of the Emissions Reduction Plan. In light of the aforementioned considerations, this study proposes the integration of a seismic resilience study into an energy system planning tool, REMix. The objective is to identify the optimal topology of electrolyzers, whether distributed, intermediate, or concentrated, to develop a framework capable of ensuring that energy systems not only transition towards sustainability but also remain resilient in the face of natural catastrophes.

1.2. Hypothesis

This study hypothesizes that the seismic resilience metrics of New Zealand's power system will vary significantly depending on the spatial distribution of hydrogen resources. Specifically, the study will compare three distinct distribution scenarios: concentrated, intermediate, and distributed.

1.3. Objectives

1.3.1. General Objective

This study aims to evaluate the resilience of the 2050 New Zealand energy system in relation to the spatial distribution of hydrogen technologies. The study conducts an earthquake resilience assessment to this end. To achieve this objective, the hydrogen demand spatial distribution scenarios, which are distributed, intermediate, and concentrated, are subjected to a comparative analysis. The study is carried out through the coupling of a resilience framework, corresponding to a probabilistic algorithm for the modeling of electrical outages related to natural disasters, with REMix, a tool for optimizing the expansion and operation of energy systems.

1.3.2. Specific Objectives

The specific objectives are as follows:

- To adapt the resilience framework to be coupled with REMix-NZ in order to simulate system operation that includes electrolyzers with untimely disconnections of generation units and transmission lines.

- To simulate the occurrence of earthquakes affecting the New Zealand electricity system in 2050.

- To assess the damage and subsequent restoration of power system components, specifically generation units and transmission lines, using fragility and restoration curves.
- To optimize the operation for three different spatial hydrogen demand distribution scenarios in order to compute resilience metrics subsequent to the occurrence of multiple events.
- To compare the spatial hydrogen demand distribution scenarios and make planning recommendations based on resilience metrics obtained from the performance of each topology.

1.4. Structure of the Document

The document is structured as follows: Chapter 2 provides a literature review of power system planning optimization tools and resilience assessments, considering the integration of new technologies. This review motivates the importance of the current study. Chapter 3 introduces the methodology for coupling resilience assessment using the power system optimization tool REMix. This chapter also delves into the resilience framework and the modeling of hydrogen in this study. Chapter 4 describes the case studies applied to New Zealand, along with the model input data and hydrogen scenarios. Chapter 5 presents the results of developing the resilience assessment in REMix for the different hydrogen demand scenarios. Finally, Chapter 6 presents the main conclusions and future research efforts.

Chapter 2

Literature Review

2.1. Energy Optimization Tools

The planning and operation of an electrical system are performed by means of an optimization process that seeks to minimize or maximize a particular variable. The complexity of the optimized system determines the type of optimization that best suits the needs. The available options include classical approaches corresponding to linear and nonlinear programming, iterative methods, probabilistic and analytical approaches, graphical construction, and approaches that are not reasonable for problems with multiple local optimums and, therefore, cannot converge to local optimums, as mentioned by the authors of [16].

When analyzing the optimization of Hybrid Renewable Energy Systems (HRES) - systems comprised of a set of technologies operating to meet electricity demand without interruptions [17] - it becomes evident that there is a need to develop optimization tools. These tools should reflect both the variability and uncertainty of variable generation technologies, as well as the inherent mathematical complexity involved in optimizing the investment and operation of a system [18]. Among the most prominent optimization software packages are HOMER, as used in research aimed at analyzing the techno-economic aspects of hydrogen in energy systems with renewable resources, such as [19], [20], TRNSYS to analyze fuel cell-based hybrid system [21], and HOGA for hybrid hydrogen and solar-photovoltaic systems [22]. These permit the optimization of HRES, including storage technologies such as batteries, hydrogen tanks, and fuel cells.

The optimization tools previously mentioned consider cost indexes such as Net Present Costs (NPC) as presented in [23], [24], Levelized cost of energy (LCOE) as used in [25], Life Cycle Cost (LCC) [26], [27], Levelized cost of hydrogen (LCOH) [28], [29], and reliability indices such as Load Power Supply Probability (LPSP) [30], [31], Expected Energy Not Supplied (EENS) [32], [33], and Level Of Autonomy (LA) [34], [35]. However, in all of the aforementioned studies where energy systems are optimized with renewable energy, these software packages do not consider resilience indices and metrics.

In the context of power system optimization, there are Python-based solvers capable of sizing and optimizing HRES as linear [36], nonlinear [37], single-objective, or multiple-objective problems [38]. One advantage of Python software is that it offers open-source packages capable of solving linear, nonlinear, quadratic, Mixed-Integer Linear Programming (MILP), and

Mixed-Integer Non-Linear Programming (MINLP) problems, among others. In the realm of linear and nonlinear problems, two notable Python-based solvers are Python for Power System Analysis (PyPSA) [39] and Framework for Integrated Energy System Assessment (FINE) [40]. PyPSA allows for linear power flow contingency analysis and security-controlled linear Optimal Power Flow (SCLOPF) [41], while FINE does not extend its capabilities to perform contingency analysis.

The REMix framework, developed by the German Aerospace Center (DLR), uses the software General Algebraic Modeling System (GAMS) to establish a linear optimization of energy system expansion and operation. This is achieved using solvers like CPLEX [43] or GUROBI [44] to solve. It was designed to facilitate the integration of renewable [42] and hydrogen technologies [45], with the objective of identifying the lowest possible cost of investment and multisectoral operation of electricity, transport, and heat [3].

2.2. Resilience in Power Systems

In the context of energy systems, resilience is defined as the capacity of a grid to anticipate, withstand, recover, and adapt its infrastructure and operation to events with a low probability of occurrence but are of high impact [46]. Consequently, a resilient energy system is one that simultaneously meets multiple characteristics. Firstly, the grid must be able to anticipate potential crises and disasters. Secondly, the resilient grid must be prepared by establishing the actions that can be deployed in critical situations and the actions that can be deployed to absorb and limit the extent of the state of degradation. Thirdly, the system must adapt and adjust its operation to respond to the undesirable situation. Fourthly, the grid must recover quickly to restore power supply and repair damage to infrastructure. Finally, there is the maintenance of critical system operation, which involves the implementation of measures to ensure the continued functioning of a reduced but functional system for everyday use [5].

The complete resilience framework of a system encompasses both pre-event estimation and post-event assessment [47], [48], as illustrated in Figure 2.1, which presents the behavior of the “state of health” over time of a system faced with a HILP event. This is referred to as the resilience curve, which clearly illustrates the system’s initial equilibrium state, accompanied by a certain level of resilience. Following the event, this resilience declines. The reduction in the system’s health results in a critical trough, after which it recovers to the initial steady state.

The resilience curve shown below graphically depicts the fair behavior of the energy system when confronted with a disruptive event. This suggests that the system returns to its initial state after the event [47], which is different from an adaptive resilience curve. The latter represents a system that compensates for the loss with performance, potentially reaching a recovery state that surpasses the initial state, but this implies a reorganization of the system [50]. In contrast, there are two distinct behaviors: ductile and collapsing. In ductile behavior, the system reaches a certain level, but its functionality is not fully restored [51]. In collapsing behavior, the system is unable to recover and loses its functionality, as described in resilience assessment studies such as [52] and [53].

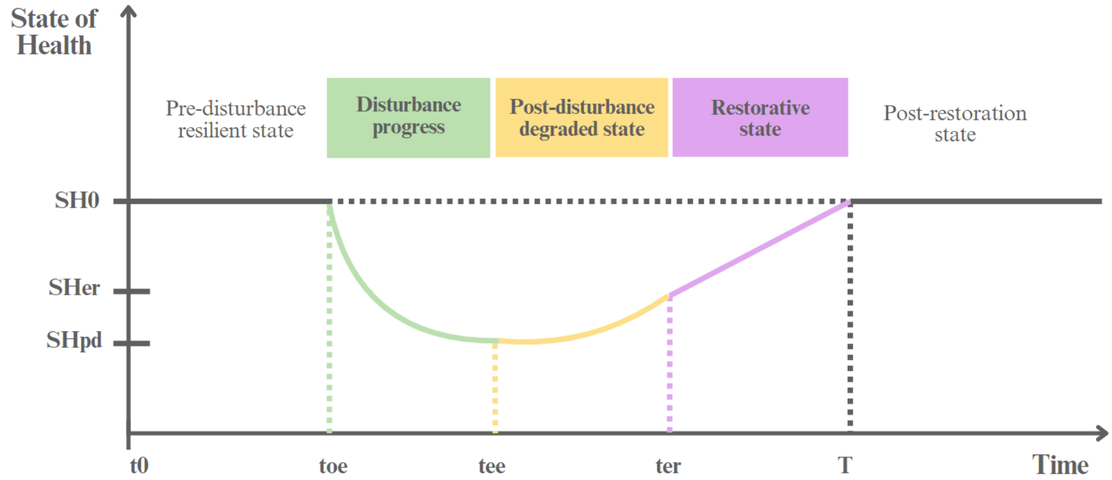

Figura 2.1: Graphic representation of a resilience curve over time. Own elaboration based on [49].

The behavior of the resilience curve may vary from system to system and may even fall outside the aforementioned categories. However, this allows for the quantification of the system's health state through a resilience indicator. This indicator can then be employed in a cost-benefit analysis of resilient planning, as evidenced in the resilience assessment exposed in [7] and the resilience metrics overview presented by the authors of [54]. Given the absence of a uniform expected behavior for a system facing a disruptive event, there is no singular methodology for quantifying resilience. This justifies the existence of multiple metrics that describe the system's operational and infrastructure resilience. In the case of operational metrics, these are designed to evaluate the effectiveness of post-event restoration measures, as outlined in references [55] and [56]. In contrast, infrastructure metrics are employed to assess the seismic vulnerability of critical components of the power system, including generators, transmission lines, and substations. Moreover, the potential for cascading failures due to interdependencies between infrastructures is evaluated, to quantify the damage resulting from the occurrence of an unexpected and catastrophic event, as shown in the resilience studies described in [56] and [57].

Given the destructive potential of events that can impact energy systems, resilience planning is crucial. Numerous studies have been conducted to develop methodologies for resilience planning and assessment. The methodology for conducting a resilience assessment, as elucidated in reference [58], suggests that the resilience analysis should be performed in stages. The authors of the [5] present a diagram that allows a more thorough examination of the steps involved in simulating hazards from a spatiotemporal perspective during the fragility modeling stage. Additionally, the authors of reference [59] provide a detailed description of the loops necessary for verifying the sequence of information required to obtain a resilience metric. Finally, the authors of references [60], [61], and [62] identify the most important outputs for resilience assessments in the final stage.

The stages of the resilience assessment, first presented in [62], include the generation of a hazard profile, the linkage of hazard intensity with the probability of damage to electrical components through fragility, and the delineation of the response and recovery functions of the system. Staged resilience assessment methodologies are employed in the context of power system expansion planning, as evidenced in [8], [63], and [64]. Transmission topology comparisons are presented in [58] applied in the electric system of Nepal; the importance of chain disconnections was emphasized, as done by the authors of [65] and [66], and the disconnections of electrical substations were analyzed according to their configuration, as done in the Chilean electrical system [67]. As evidenced by [68] and [69], distribution network evaluations and assessments of new technologies, such as storage units [70], are employed to identify the optimal configuration responsive to the analyzed hazard.

Hazards may include natural disasters such as earthquakes, as evidenced in multiple studies, such as the network planning study exposed in [7], the decision-making algorithm detailed in [8], the damage cascading analysis made in [65], the optimization via simulation developed in [67] to improve the seismic resilience of power systems and the electrical substations damage assessment presented in [71]. Furthermore, the effects of volcanic activity [72] and extreme weather conditions, such as typhoons [73] and extreme wind variability [74] are considered in other studies, attempting to minimize load loss through proactive generation dispatch decisions. It should be noted that the resilience assessment methodology exposed in the literature is sufficiently generic to allow for the parameterization of all types of events.

Among the potential threats to be considered when analyzing the impact of HILP events on electrical grids, many studies evaluate the occurrence of earthquakes. The authors of multiple resilience assessment studies, such as the network planning presented in [7] and [8], besides the electric systems components damage analysis detailed in research [67] and [75]; propose optimization models to design investment plans that mitigate and reduce the impact of earthquakes, which are particularly noteworthy. This study underscores the importance of distinguishing between planning a reliable grid and a resilient grid. The former anticipates frequent low-impact events, ensuring that these do not disrupt the infrastructure and operation of the network each time they occur.

The evaluation of an electrical network's resilience, or state of health, is materialized in the computation of resilience metrics. Some authors classify these metrics as performance-based and non-performance-based [54]. They highlight that the former correspond directly to the output quantity of a power system, so they are obtained directly from the prediction of the system behavior, for example, through Monte Carlo simulations. In contrast, non-performance-based metrics are employed to identify factors that may affect the system before, during, and after an event. These metrics are derived from on-site visits and damage statistics obtained from previous events. In the case of earthquakes, the resilience metrics that stand out are performance-based and mainly calculate the energy not served, which is the total amount of electrical energy not delivered to consumers [67], and unsupplied load, the instantaneous power demand that cannot be met at a given moment, representing the immediate shortfall in power supply [76] [77].

A noteworthy resilience metric in the context of earthquake assessment is the FLEP metric. The FLEP metric system for power system resilience is a set of four metrics defined to quantify the state of health of a power system. These metrics are explained in [78], and used in seismic resilience assessments such as [7] and [67]. The FLEP metrics represent the rate of decline in resilience (Φ) and the severity of the decline (Λ) during the Disturbance Progress Phase, as illustrated in the resilience curve (see Figure 2.1). They also encompass the extent (E) of the post-disturbance degraded Phase and the speed (Π) with which the network recovers to its pre-event resilient state at the end of the Restorative Phase.

2.2.1. Planning for Resilience Energy Systems with Hydrogen

As previously stated, resilient energy system planning primarily considers the expansion of generation and transmission and the significant integration of new technology into the system. In particular, the integration of hydrogen can be highlighted as a beneficial strategy, particularly in terms of providing flexibility to the system. This is achieved by diversifying the available technologies, allowing hydrogen to be generated during periods of low demand or high renewable production, and then stored for deployment in the event of an extreme contingency [10]. The references [79] and [80] present studies that analyze the resilience of hydrogen integration into an energy hub and the system's operational performance. Other studies focus on improving resilience in distribution networks that include hydrogen systems [81].

2.3. Hydrogen Planning in Energy Systems

In the context of the global energy transition and the diversification of energy matrices in the world's electricity systems, in research conducted in New Zealand [15], Australia [82], the European Union [83], and Colombia [84], hydrogen emerges as a promising energy vector capable of providing the systemic flexibility required to achieve the decarbonization and carbon neutrality objectives outlined in numerous national global strategies. Consequently, its extensive integration must be carefully planned, taking into account a multitude of factors. From the planning of pink hydrogen [85] or gray hydrogen [86], the determination of storage availability on hybrid systems, such as the references [87] and [88], to the study of mathematical aspects of the optimization that considers the integration of hydrogen into the energy system [89], this planning is of great importance. It must consider the investment and operating costs of this technology in the system, but also its production and other externalities such as carbon emissions and environmental damage that its massive integration produces in the environment.

2.4. Overview of the Geographical and Electrical System Context of New Zealand

2.4.1. Natural Hazards and Threats

New Zealand, owing to its geographical location and topography, is prone to various natural disasters and extreme weather events. These include earthquakes, tsunamis, volcanic activity, thunderstorms, floods, and droughts, as documented in the available literature on these phenomena in the country, such as [90], [91], [92]. The Climate Change Knowledge Portal categorizes these events into two groups: frequent but low-impact and infrequent but high-impact (HILP) events.

From 1980 to 2020, statistical data reveals that New Zealand encountered 22 flood events, affecting an average of 1,300 people in each instance. These occurrences, while frequent, have a relatively low impact. On the other hand, earthquakes, which occurred five times during the same period, are infrequent but significantly impactful. These events affected an average of 125,500 people [93]. The Canterbury and Kaikoura earthquakes in 2010/2011 and 2016 were notably the most destructive [92].

The country's location on the boundary of the Pacific and Australian tectonic plates is a primary contributing factor to the high number of earthquakes experienced by New Zealand each year. Of these earthquakes, approximately 200 are of sufficient intensity to be felt [90] [91]. While earthquakes can occur anywhere in New Zealand, according to data from the Earthquake Commission (EQC), zones of increased seismic risk cross-cut the country's North and South Islands [94]. In particular, the Canterbury region has been identified as having approximately 100 known faults, with Rangiora-Cust, Hororata, and Darfield being the most earthquake-prone areas [95].

The historical record of earthquakes in New Zealand is extensive, with a wide range of magnitudes. One of the most recent and disturbing events, with a magnitude of 7.3 on the Richter scale and a depth of 20 km, occurred in Gisborne in the year 2021. The magnitude of the earthquakes that have occurred in New Zealand varies considerably. For example, the earthquake that occurred in January 2010 had a magnitude of 7.3 on the Richter scale and a depth of 20 km. This was followed by aftershocks in 2010/2011, whose magnitudes fluctuated between 5.0 and 7.0 degrees Richter and with depths between 1 and 38 km [96].

2.4.2. Energy System

New Zealand's electricity system is distinguished by its high level of renewable energy, with 7.4 GW of the total 9.4 GW installed capacity derived from renewable sources. The predominant technology in the system is hydroelectric, with 5.4 GW installed, followed by fossil fuel generation with gas, coal and diesel, which together account for 2.2 GW, followed by wind and geothermal energy with 1.3 and 1.2 GW, respectively [11]. This production allows for the supply of electricity to meet demand, which in 2023 was 35 % from the industrial sector (mining, food processing, wood, pulp, paper, and graphic arts, chemicals, basic metals), 33 % from residential demand, 24 % from the commercial sector, 6 % from agriculture, forestry, and fishing, and only 0.5 % of the demand came from the transportation sector [97].

New Zealand generated 39.6 terawatt-hours (TWh) of electricity in 2022. Of this total, 22.3 TWh was generated in the North Island and 18.4 TWh in the South Island. In contrast, demand was distributed as follows: 23.6 TWh in the North Island and 16.0 TWh in the South Island. Consequently, the system's operation is predicated on the HVDC interconnection between islands, which ensures the supply of northern demand with southern generation [97].

In addition to the electricity system, when the energy sector as a whole is analyzed, it becomes evident that the system maintains a dependence on fossil fuels. In fact, 60.51 % of the energy demand was supplied with natural gas, with the industrial sector concentrating 75.87 % of the demand [97]. Public policies have been developed in response to the above, including the Climate Change Response Amendment (Zero Carbon) Act of 2019. This Act mandates that net emissions of all greenhouse gases (except biogenic methane) be reduced to zero by 2050 and that biogenic methane emissions be reduced by 24 % to 47 % below 2017 levels by 2050, including 10 % below 2017 levels by 2030 [98], [99].

The Zero Carbon Act establishes a key point regarding the requirements for the government to develop and implement climate change adaptation and mitigation policies. This justifies the need for a planned energy transition, considering the national goals that are also reflected in the energy strategies, which have two main focuses: The New Zealand Gas and Hydrogen Transition Plan and the New Zealand Energy Strategy [100].

New Zealand's hydrogen strategy represents a key element of the country's broader efforts to develop an industry capable of reducing emissions, maximizing economic benefits, and ensuring energy security and resilience [101]. A pivotal element of New Zealand's Energy Strategy is the Hydrogen Roadmap, which delineates the government's objectives for this energy vector. The roadmap anticipates a significant increase in demand for green hydrogen, with up to 560,000 tonnes per year by 2050. It also emphasizes the importance of investment in electrolyzers and the expansion of renewable electricity generation by at least 12.5 GW by 2050 [15]. One of the advantages of planning and expanding hydrogen production is the projected 3.8 to 8.2 terawatt-hours of demand response capacity and 1.56 to 2.26 trillion liters of displaced liquid fuel between 2022 and 2050. This would strengthen energy resilience and security.

Table 2.1 presents a summary of the key literature review, with the objective of contrasting the research analyzed with the work done in this study.

2.5. Contribution

This study represents a pioneering analysis of resilient power system planning in New Zealand. The study compares large-scale concentrated and small-scale decentralized hydrogen resources throughout the network using the REMix energy system modeling framework. The research goals addressed here are of critical importance for several reasons.

Firstly, in a country undergoing a rapid transition towards renewable energy sources, the implementation of resilient planning strategies utilizing optimization tools such as REMix is of paramount importance. This is of particular importance in light of the increasing frequency of severe weather events and natural disasters, which necessitate the implementation of proactive measures to ensure the power system's ability to withstand, recover, and adapt its operation and infrastructure.

Secondly, the role of hydrogen as an energy vector is evident, showing its potential to enhance system flexibility. Its integration into energy frameworks as a demand presents technical challenges, necessitating a planned and strategically implemented approach.

Overall, this research contributes to the understanding and advancement of resilient power system planning, taking into account the specific characteristics and challenges of the New Zealand context.

Table 2.1: Summary of the main literature review.

Reference	Main Contributions	Case Study	PV Wind	Stor	H2	Detailed Res FWK	Infra Res Metric	Oper Res Metric
[8]	Two optimization models are proposed: one for ensuring network reliability in the event of internal failures, and another for enhancing resilience in the face of external disasters.	IEEE 14-bus case study, wherein a variety of resiliency strategies are analyzed, including the addition of new lines, the enhancement of seismic resistance in buses, and the incorporation of distributed generation.	✓	No	No	✓	✓	No
[82]	Evaluate the resilience of energy hubs (EHs) to extreme events such as hurricanes using a stochastic mixed-integer linear programming model that accounts for uncertainties in damaged transmission lines.	IEEE 24-bus power system with an EH on bus 14. The EH draws fuel from a gas network and exchanges power with the system. It includes a cogeneration unit, generator, electrolyzer, boiler, thermal storage, and heat storage to meet electrical, thermal, and hydrogen demands.	✓	✓	✓	No	No	No
[83]	Analyze how operational resilience is integrated into capacity expansion models for green hydrogen production via hybrid renewable energy systems (HRES). The function used considers climate variability in plant siting decisions and compensates for it with batteries and hydrogen tanks.	Regional-scale case study is to ascertain whether the system can be considered operationally resilient if it possesses sufficient autonomy to withstand non-catastrophic unfortunate events. In order to achieve this, it is necessary to enhance the system's storage capacity and reduce its reliance on wind energy sources.	✓	✓	✓	No	No	✓
[84]	Examine the potential of utilizing hydrogen systems to enhance the resilience of distribution networks through the implementation of cost-effective long-term energy storage solutions.	The case study comprises a validation of H2 systems on an IEEE 33-node distribution network, with six PV units and three H2 systems hosted by network.	✓	✓	✓	No	No	No
[92]	Development of an optimal electricity-hydrogen integrated energy system (EH-IES) planning strategy. This paper presents an innovative model that combines battery energy storage and hydrogen storage to optimize renewable energy management and meet electricity, heat, and hydrogen demand.	Examines the regional energy supply with minimal carbon emissions, powered by renewable energy sources. It is designed to supply hydrogen for fuel cell forklifts in nearby factories, alongside electricity and domestic hot water.	✓	✓	✓	No	No	No
This research	Presents a methodology for the earthquake resilience power system planning of a national network, which considers the integration of hydrogen resources.	Present a representative scheme of New Zealand's 11-node renewable energy infrastructure, incorporating storage technologies.	✓	✓	✓	✓	✓	✓

Chapter 3

Methodology

This chapter describes the framework developed to analyze the resilience of a national power system using an energy optimization tool. The coupling of the resilience study to the REMix energy optimization tool is first explained. Then, the stages that constitute a resilience study and the configuration of the optimization model are described in detail. Finally, the hydrogen demand scenarios that enable the construction of the case studies are presented.

3.1. Overview

Figure 3.1 shows the proposed modeling approach, presenting in a general way the model inputs, corresponding to the topology of the system analyzed according to each hydrogen demand scenario and to the parameters that describe a natural disaster that can introduce disturbances to the electric system, which are characterized using the fragility curves and the restoration curves of the electric components. On the other hand, random processes are indexed, which correspond to the occurrence of a natural disaster and the operation of the system before its occurrence. Finally, the outputs of the model are the system disconnection profiles, the operation of the system after the occurrence of a natural disaster, and the measurement of resilience through the computation of a metric.

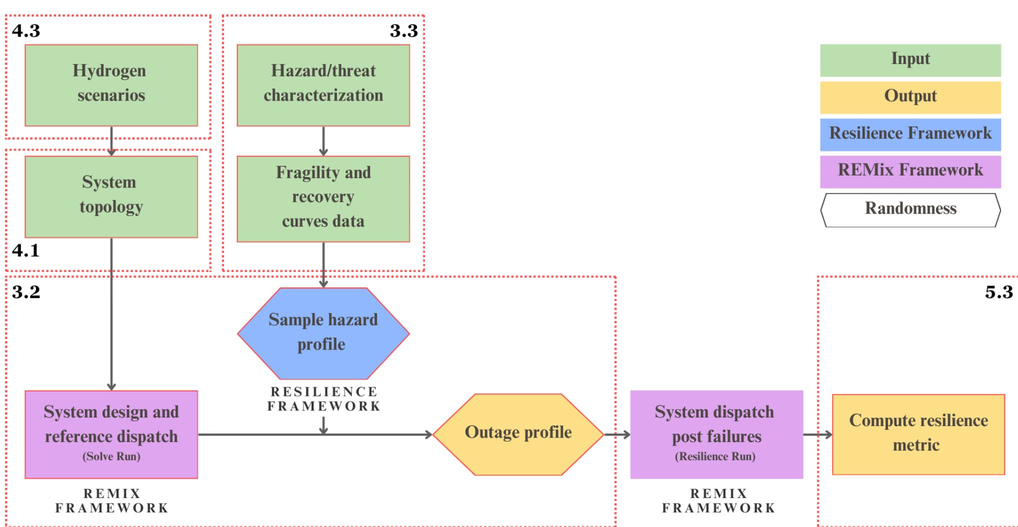

Figura 3.1: General modeling approach. The numbers below refer to the subsections where detailed information is provided.

3.2. Modeling Approach

The study presented in this study focuses on developing a three-stage model, as shown in Figure 3.2. Within this model, the 4-phase resilience assessment will be carried out. The initial stage involves *Fragility Modeling*, which presents the system's topology and operation before any disturbances occur. Data is collected to characterize natural hazards and describe potential damage and later restoration of the electrical system components through fragility and restoration curves.

The second stage includes *Failure Simulations* that randomly select parameters describing a natural hazard to calculate the probability of damage to each component of the electric system. Based on this probability, capacity reduction determining disconnection profiles is established, subsequently influencing the system's operation after faults. Therefore, using disconnection profiles allows for assessing the system's response in terms of infrastructure and capacity loss to meet demand.

The final stage encompasses calculating *Resilience Metric* following adequate testing; these metrics represent average energy not supplied due to disconnections caused by natural hazards.

3.2.1. REMix Energy Optimization Tool

The optimization tool used for this study corresponds to REMix [3], an energy system modeling framework initially developed by the German Aerospace Center (DLR) and limited to the electricity sector but extended to couple the transportation and heating sectors to obtain a tool to evaluate future scenarios based on a system with high spatial and temporal resolution.

REMix (Renewable Energy Mix) is a deterministic linear optimization program implemented in the General Algebraic Modeling System (GAMS) and solved with CPLEX. The program has a multi-nodal approach, where nodes can be connected by different transport infrastructures. In each region, all units of a given technology are aggregated and treated as a single unit.

The program allows the analysis of system capacity expansion and hourly operation over the entire time horizon, which is comprehensively optimized in a single run. REMix minimizes the investment cost of technologies, the amortization time, and the investment rate for expanding generation, transmission lines, and storage capacity according to the system requirements and potential availability.

The general structure of REMix is shown in Figure 3.3, where the input information and model outputs are identified.

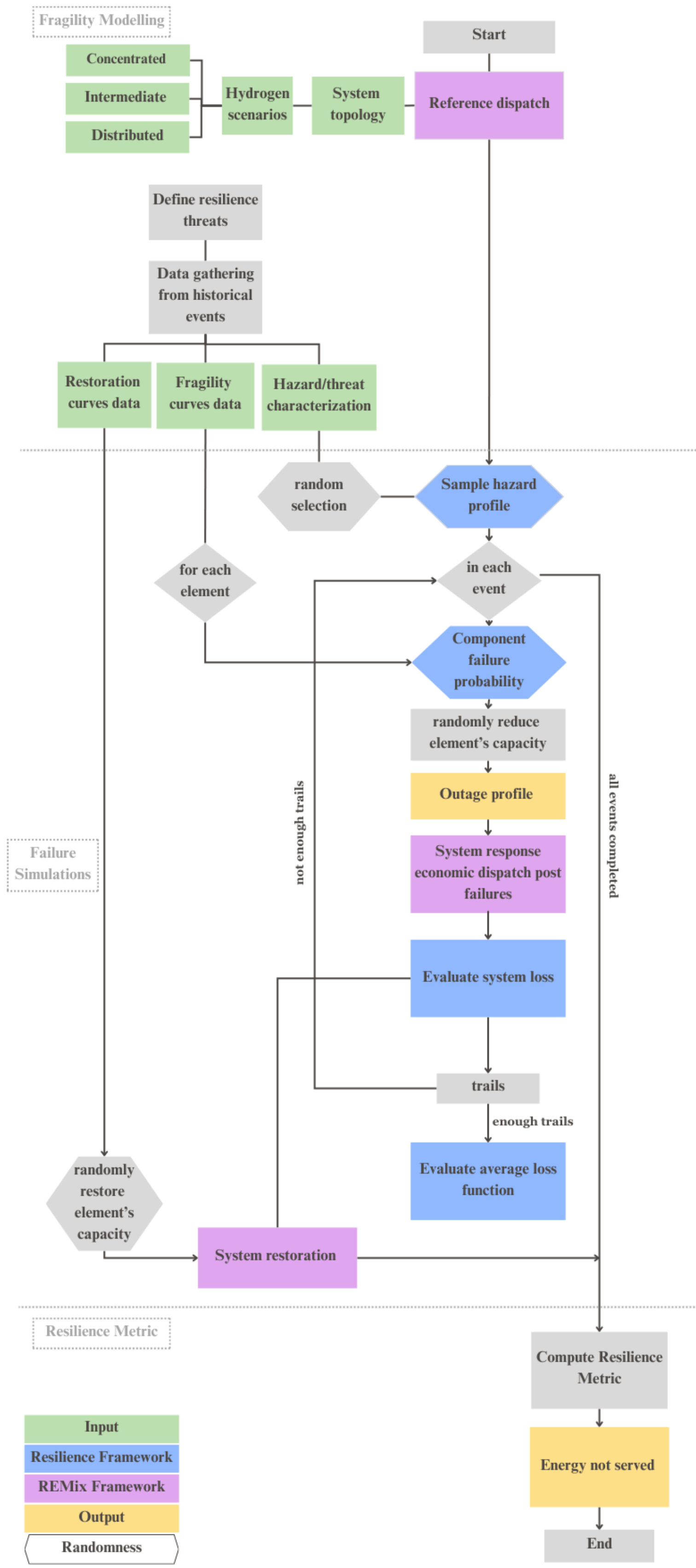

Figura 3.2: Detailed methodology flowchart. Own elaboration using as model the resilience assessment methodologies presented as diagrams in the references [5], [58], [59], [60], [61] and [62].

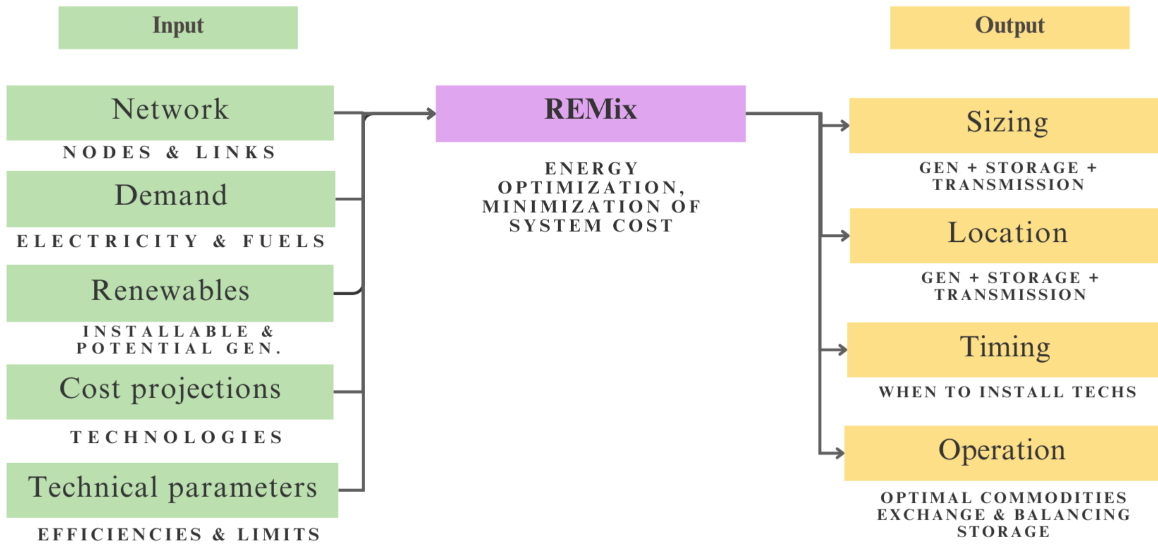

Figura 3.3: REMix optimization tool flowchart with basic components.

3.2.2. REMix - Resilience

The REMix - Resilience tool developed in this study corresponds to an adaptation of the original framework to introduce generation technologies, transmission lines, and demand outage profiles. Thus, the optimization is modified to be performed in two consecutive runs [102]:

Solve Run: The system expansion is performed, i.e. it is decided by the installed capacities for each technology in the year 2050, taking into account the availability of resources and the minimization of the investment and operating costs of the system. This optimization aims to build the system and obtain the base case to understand how the system operates under normal conditions.

Resilience Run: the optimization is limited so that only the operation optimization is performed, that is, without expanding the system and considering the introduction of shutdown profiles through an additional parameter corresponding to a functionality time series. Thus, the system is operated to analyze its response to the disconnection of generation, transmission, and demand due to the occurrence of an extreme and unforeseen event. Thus, the system is operated to analyze its response to the disconnection of generation, transmission, and demand due to the occurrence of an extreme and unforeseen event.

From the contrast between the first run, under normal conditions, and the second run with technology disconnections, corresponding to the "Resilience Run", it is possible to calculate a resilience metric, either on the infrastructure and energy demand not served due to the contingency associated with the occurrence of the extreme event.

In practice, the generation, transmission, and demand shutdown profiles are introduced by setting the parameter for generation and transmission equal to 0 from the beginning of the year until the time of the event. Then, from the time step until the decision to restore the system, a parameter greater than 0, where 1 is the loss of 100 % of the capacity, is set to indicate the percentage of disconnection for each technology.

On the other hand, the change in the demand profile is determined by setting a parameter of 0 from the beginning of the year until the event occurs and then setting a number less than 0, where -1 is the loss of 100 % of the demand, to indicate the loss of disconnection for each type of demand.

3.3. Resilience Framework

The resilience assessment conducted in this study consists of four main phases, as first presented in [62]:

Hazard characterization: Historical data is used to generate thousands of scenarios, each providing information on the intensity and spatio-temporal description defining the occurrence of a natural disaster.

System component vulnerability evaluation: Fragility curves are utilized to determine the probability of disconnection for each electrical system component at a given intensity of the natural disaster. This information is then used randomly to define the percentage of disconnection.

Electrical system response: This phase analyzes how the operation is reorganized among available electrical units in the network after generation and transmission units are disconnected due to a natural disaster.

Electric system recovery: The optimization considers infrastructure and operational restoration using restoration curves.

3.3.1. Earthquake Characterization

Earthquakes are high-impact, low-probability events that can damage electrical systems. Due to their unpredictable nature, they are associated with high uncertainty. The damage caused by earthquakes to each system component is determined randomly by fragility curves.

After an earthquake with a well-defined epicenter (latitude and longitude) and intensity and depth, it is possible to characterize this natural hazard and its impact on the electrical system by calculating the maximum ground acceleration (PGA) at each point where an electrical component is located. Therefore, the PGA is a parameter that characterizes earthquakes based on the amount of ground shaking they introduce. This allows for assigning a measure of intensity to the natural hazard, determining the probability of electrical components being damaged due to such an event.

The Peak Ground Acceleration (PGA) [103], measured in gals, is calculated using the equation 3.1:

$$PGA(r,h,M) = \frac{e^{-2.73\ log(r+1.58\ exp(0.608 \cdot M))} \cdot e^{6.36+1.76 \cdot M+0.00916 \cdot h}}{980.665} \tag{3.1}$$

where M is the magnitude intensity of the earthquake on the Richter scale, h is the depth of the earthquake determined by the hypocenter (ex, ey, h), and r is the radius that determines the distance between the epicenter (ex, ey) and the location (x, y) of a given electrical component, calculated according to the equation 3.2:

$$r = \sqrt{(ex - x)^2 + (ey - y)^2} \tag{3.2}$$

3.3.2. Vulnerability Assessment

Assessing an electrical system component's vulnerability to unexpected high-impact events determines the extent of its structural damage. Earthquakes can be instantaneously disruptive, causing significant perturbations in the system.

Fragility curves enable the prediction of the potential damage state of an electrical component based on specific event parameters and geographical location. The PGA is calculated for each electrical component in its specific position according to the earthquake's defined intensity and hypocenter. This calculation allows for determining the probability associated with each damage state (complete, extensive, moderate, and slight) by comparing the likelihood of a given damage state to another previously graphically defined state.

Fragility curves can be derived from empirical data through statistical analysis of observed years, analytical determination based on a specific simulation model, or experimental determination through deliberate component failure. Figure 3.4 presents the fragility curves of generation units and high-voltage electrical substations used in this study. The curves are based on information from the HAZUS manual [9], which describes the behavior of the units according to lognormal distribution functions. These functions provide the probability of reaching or exceeding different damage states given a specific PGA.

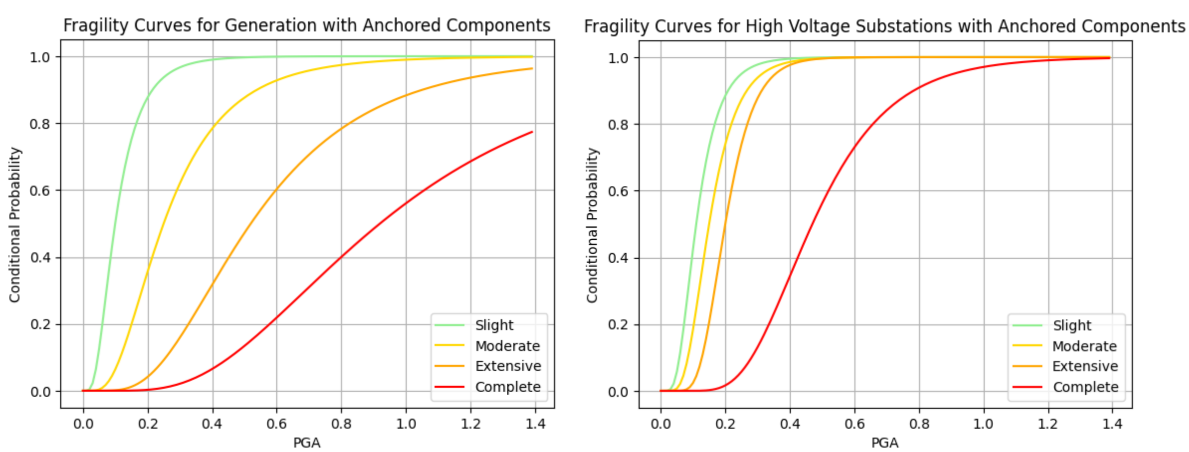

(a) Fragility curve for generation units.

(b) Fragility curve for electric substation.

Figura 3.4: Fragility curves for power system components Own elaboration based on the data presented in [9].

3.3.3. Restoration Data

The restoration of each electrical component's total capacity is determined by the recovery curves, which describe the time it takes to recover from the damage caused by the earthquake. These curves are modeled as a normal distribution function, as shown in Figure 3.5, based on information from the HAZUS Earthquake modeling manual [9].

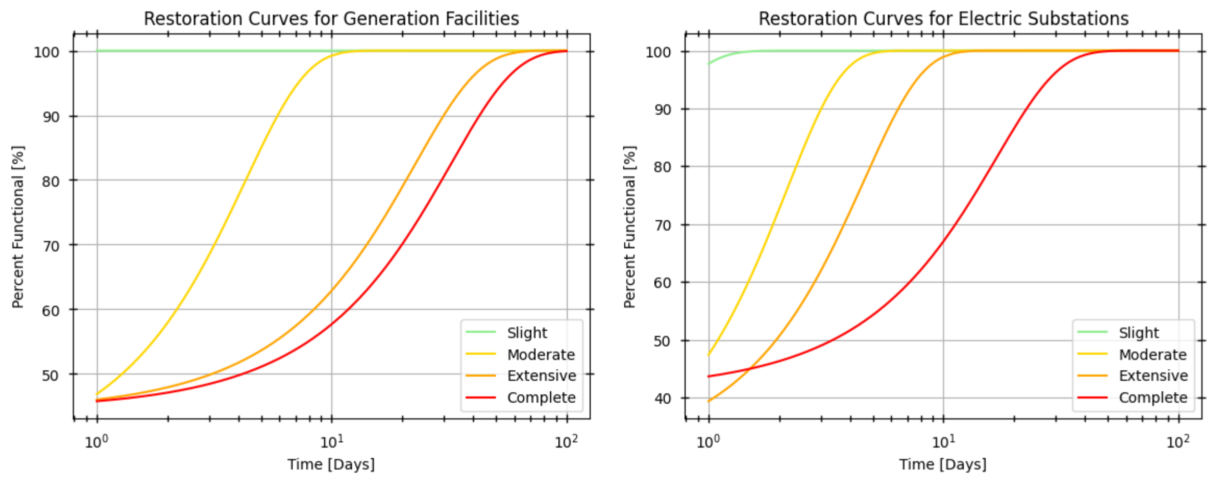

(a) Restoration curve for generation units. (b) Restoration curve for electric substation.

Figura 3.5: Restoration Curves for power systems components. Own elaboration based on the data presented in [9].

The information in the HAZUS manual for earthquake modeling, although based on U.S. experience, is justified for modeling damage to electrical components of the New Zealand electrical system for several reasons. Firstly, as stated in the manual itself, the methodology is robust, as it considers numerous variables and scenarios to construct the fragility and restoration curves, which makes it adaptable to other contexts.

Furthermore, the lack of specific local information provides an additional justification. While there are studies on fragility and restoration curves for earthquakes in New Zealand, these primarily focus on buildings [104] and not on electrical components beyond cables [105].

At last, earthquake engineering principles exhibit considerable universality. The intrinsic behavior of structures and systems impacted by seismic events displays only minor regional disparities. As a consequence, the knowledge acquired by HAZUS can be deployed globally.

3.3.4. Resilience Metrics

To evaluate the electricity system's resilience within the framework of hydrogen production, specific metrics have been selected based on outcomes from optimizing the system operation on REMix. The FLEP metric [78] gauges infrastructure and demand resilience by examining how the connected generation and demand curves behave over time. Additionally, unserved energy is quantified as the disparity between demand and generation output obtained directly from REMix runs. This performance measure indicates that a more resilient system experiences minimal unserved energy during HILP events.

The indicators applicable to earthquake occurrences are L, E, and P. These time-dependent metrics are employed to assess the resilience of a system in the context of an earthquake. The initial metric, L, addresses the question of "how *low* is the state of health of the system?" and corresponds to the percentage reduction between the pre-event and lowest capacity after the event. E reflects the *extent* of the disturbance state and corresponds to the number of hours the unfavorable state extends. P measures how *promptly* the system resilience levels recover, i.e., capacity recovery over time.

In quantitative terms, each of the LEP metrics can be calculated by considering the resilience curve presented in Figure 2.1. L corresponds to the difference between the initial health state and the lowest health state experienced by the studied variable during the disturbance progress. Thus, the equation 3.3 is used to calculate the metric L:

$$L = SH_0 - SH_{pd} \tag{3.3}$$

The metric E is calculated as the time in which the system remains in the post-disturbance degraded state, according to the equation 3.4:

$$E = t_{er} - t_{ee}. \tag{3.4}$$

Finally, the metric P is obtained by calculating the pendency of the restorative state, according to the equation 3.5:

$$P = \frac{SH_0 - SH_{er}}{T - t_{er}} \tag{3.5}$$

3.3.5. Earthquake Resilience Assessment

The methodology for evaluating the resilience of power systems to seismic events involves a multi-step process, which is detailed as follows and as presented in Figure 3.6:

1. Initialization of Seismic Variables: Commences with the random selection of seismic event characteristics such as the epicenter, intensity, and time of occurrence.

2. Peak Ground Acceleration Determination: Involves calculating the PGA at the locations of all system generators and at each system node.

3. Damage Assessment Based on Fragility Curves: Employs the fragility curves of generation units and electrical substations to ascertain the damage extent to each generator and node probabilistically. Assumes that a damaged node causes a proportional loss of capacity to all connected components, thus affecting transmission lines and demand.

4. Restoration Curve Analysis: Utilizes the restoration curves to estimate the timeframe required for system components to regain total operational capacity after damage.

5. Formulation of Disconnection and Reconnection Profiles: Develop specific profiles for the disconnection and subsequent reconnection of each generation technology, transmission line, and nodal demand.

6. Resilience Analysis through REMix: The generated profiles are provided as inputs to the REMix tool, enabling the analysis of the system's resilience against the seismic event.

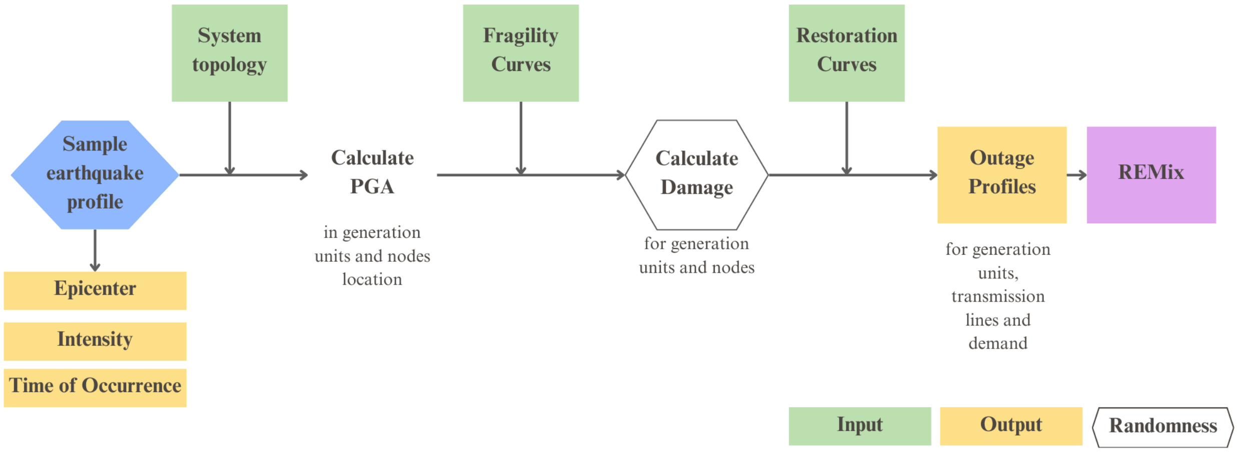

Figura 3.6: Earthquake resilience assessment flowchart.

Chapter 4

Case Study and Data

This case study aims to assess the performance of three hydrogen demand configurations in New Zealand for the year 2050 in the event of earthquakes. The configurations include concentrated, intermediate, and distributed demand, as will be outlined in Section 4.3.

4.1. REMix for New Zealand

REMix-NZ is an integrated multi-energy system model for New Zealand that includes the electricity, heat, transport, and industrial sectors. The model is based on the open-source framework REMix, developed by the German Aerospace Center (DLR). REMix-NZ allows for linear deterministic optimization with hourly resolution of the New Zealand system, which is organized into 11 geographical regions and includes almost 100 energy technologies. Figure 4.1 shows the organization of the New Zealand regions in REMix-NZ.

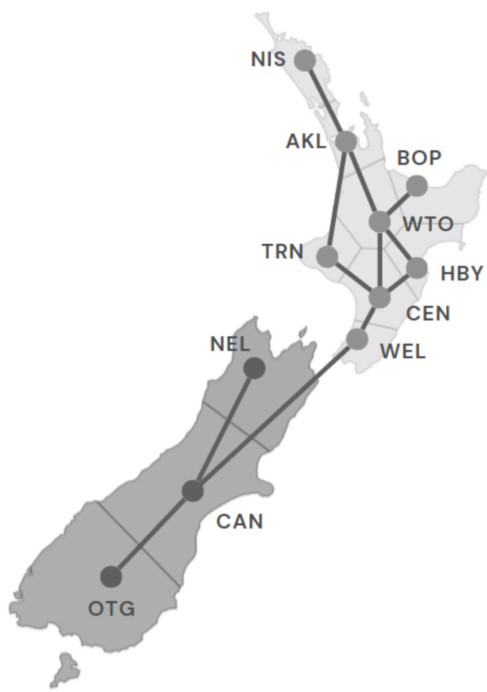

Figura 4.1: New Zealand REMix-NZ representative scheme.

4.1.1. REMix-NZ for 2050

4.1.1.1. System Expansion 2050

In this study, REMix NZ is utilized solely for the electricity sector. The system expansion for 2050 is carried out based on the annual demand by region as detailed in Table 4.1. The available technologies for expansion include PV (central fixed, central track azimuth, and decentralized), wind (onshore, offshore floating, and offshore foundation), gas (gas turbine, combined cycle gas turbine, and open cycle gas turbine), thermal (biomass, diesel, and coal), batteries, and electrolyzers. In addition, the model takes into account the performance of the operation of geothermal and hydro units in the power system, excluding any potential expansion.

Table 4.1: Projection of the electric demand by region for New Zealand in the year 2050.

Region	Electricity Demand [TWh/year]
AKL	20
BOP	6.5
CAN	16
CEN	4.9
HBY	4.4
NEL	3.0
NIS	4.8
OTG	21
TRN	2.2
WEL	7.2
WTO	8.5
Total	99

4.1.1.2. Generation Parameters

Table 4.2 presents the installed capacity in the New Zealand electricity system as of March 2024 [11], classified by technology and model region. The acronyms GT, CCGT, and OCGT represent gas turbine, combined cycle gas turbine, and open cycle gas turbine, respectively.

Table 4.3 illustrates the potential for the expansion of solar and wind generation technologies in the model regions. The technologies not included in the table are those that lack expansion capacity, such as geothermal and hydro, or possess infinite expansion capacities, such as gas, thermal, batteries, and electrolyzers.

Table 4.2: Installed generation capacity of the New Zealand power system in 2024.

Tech	Region											Total [MW]
	AKL	BOP	CAN	CEN	HBY	NEL	NIS	OTG	TRN	WEL	WTO	
Wind	-	-	-	522	-	1	-	111	133	223	64	1,054
Geoth	-	175	-	-	-	-	25	-	-	-	836	1,036
Hydro	-	247	1,717	414	149	76	5	1,793	41	-	1,015	5,457
GT	179	37	-	-	-	-	-	-	439	10	804	1468
CCGT	-	-	-	-	-	-	-	-	-	-	385	385
OCGT	55	10	-	-	155	-	-	-	435	-	92	747
Biomass	16	-	3	-	-	-	10	-	-	4	5	37
Diesel	-	-	-	-	-	3	18	-	-	-	-	21
Coal	112	-	-	-	-	-	-	-	-	-	-	112
Total	361	469	1,721	935	304	81	58	1,904	1,048	237	3,201	10,318

Table 4.3: Potential installable capacity for each technology per model region for 2050.

Tech	Region											Total [GW]
	AKL	BOP	CAN	CEN	HBY	NEL	NIS	OTG	TRN	WEL	WTO	
PV Central Fixed	181	238	1,084	497	259	477	240	1,165	156	153	387	4,837
PV Central Track Azimuth	181	238	1,074	497	259	476	240	1,153	156	153	387	4,814
PV Decentral	2	1	1	1	0	0	0	0	0	1	1	8
Wind Offshore Floating	35	22	68	6	16	93	47	157	71	15	15	543
Wind Offshore Foundation	13	6	25	2	6	13	5	10	9	1	2	91
Wind Onshore	8	11	32	17	10	15	10	35	7	6	15	166
Total	418	515	2,285	1,019	550	1,074	542	2,520	398	329	806	10,458

Table 4.4 presents a comprehensive overview of the investment costs (CAPEX) and fixed (OPEX Fix) and variable (OPEX Var) operating costs associated with all available technologies for the New Zealand power system expansion in 2050, along with the estimated useful life and CO2 emissions cost.

Table 4.4: Costs and emissions by generation technology.

Tech	CAPEX [€/kWel]	OPEX Fix [€/(kWel a)]	OPEX Var [€/kWel]	Lifetime [years]	CO2 Emissions [€/tCO2]
PV	166	3.70	0	40	0
Wind	900	18	0	25	0
Geothermal	3610	80	0	40	0
Hydro	1650	49.5	0.003	50	0
GT	475	14.25	0.011	35	150
CCGT	775	19.38	0.002	35	150
OCGT	475	14.25	0.011	35	150
Biomass	1830	32.9	0.004	25	150
Diesel	830	27.9	0.004	30	150
Coal	1600	20	0.001	45	150
Battery	61	1.71	0	20	0
Electrolyzer	350	2.59	0	35	0

4.1.1.3. Energy Not Served

In this model, the cost of unserved electricity, termed Slack Cost, is set at 3 million euros per gigawatt-hour (GWh), while the cost of unserved hydrogen demand, or H2 Slack Cost, is set at 1.5 million euros per GWh. This cost structure prioritizes the supply of electricity over hydrogen in contingency scenarios.

The rationale behind this is that the economic impact of not supplying hydrogen is lower compared to that of supplying electricity. Therefore, the model will select the less costly option of not serving hydrogen when faced with supply constraints. If the consequences of unserved demand were more severe, it is possible that both electricity and hydrogen supplies would be compromised. It is therefore crucial to highlight this prioritization in order to facilitate understanding of the model's decision-making process under various scenarios.

4.2. Earthquakes in New Zealand

The simulated extreme event is an earthquake with a magnitude of 7.8 on the Richter scale and a depth of 5 km. This magnitude and depth were chosen to represent a significant seismic event with the potential for widespread impact, based on historical data. A depth of 5 km is representative of a shallow earthquake, which typically results in significant ground shaking and damage.

The epicenters of the simulated earthquakes are distributed uniformly across the 11 regions representing New Zealand. This approach ensures that the simulation accounts for the possibility of an earthquake occurring in every electrical node within the representative scheme of the country, providing a comprehensive assessment of potential impacts across every model region. Table 4.5 displays the epicenters chosen for this study, illustrating the geographical spread and ensuring that the analysis covers a wide range of scenarios.

Table 4.5: Set of parameters and earthquake epicenters with uniform distribution for event simulation.

Region	Number of Earthquakes	Magnitude	Depth [km]	epi_x [°]	epi_y [°]
AKL	46	7.8	5	-36,95	174,86
BOP	46	7.8	5	-37,99	176,83
CAN	45	7.8	5	-43,86	171,34
CEN	45	7.8	5	-40,28	175,64
HBY	46	7.8	5	-39,55	176,82
NEL	45	7.8	5	-41,67	172,87
NIS	45	7.8	5	-35,88	174,47
OTG	46	7.8	5	-45,48	169,32
TRN	46	7.8	5	-39,33	174,32
WEL	45	7.8	5	-41,15	174,98
WTO	45	7.8	5	-38,42	175,80

The earthquake's occurrence time is determined by simulating the operation of the New Zealand electricity system without any event, i.e., the first "Solve Run", and identifying the period of maximum marginal costs. The earthquake happens during the 4900th hour of a simulation year, corresponding to a June day at approximately 1 p.m. The day in question was selected on the basis of its high energy cost, which was determined through the optimization of the system without the occurrence of any disruptive event.

4.2.1. Fragility Curves Data

The fragility curves of the generation units and electric substations (connection nodes) are obtained by employing the cumulative probability density function for a lognormal distribution, utilizing the data presented in Table 4.6 [9].

Table 4.6: PGA Fragility Functions for generation units and electric substations.

Component	Damage State	Median (g)	β
Small Generation Units (less 100 MW)	Slight	0.1	0.6
	Moderate	0.2	0.6
	Extensive	0.5	0.5
	Complete	0.8	0.5
Large Generation Units (more than 100 MW)	Slight	0.1	0.6
	Moderate	0.3	0.6
	Extensive	0.5	0.6
	Complete	0.9	0.6
High Voltage Substations	Slight	0.1	0.5
	Moderate	0.2	0.5
	Extensive	0.2	0.4
	Complete	0.5	0.4

4.2.2. Restoration Curves Data

The recovery curves for the generation units and electrical substations (connection nodes) are obtained by employing a normal distribution function with the data presented in Table 4.7 [9].

Table 4.7: Restoration Functions for Electric Power System Components.

Component	Damage State	Median (days)	σ (days)
Generation Facilities	Slight	0.5	0.1
	Moderate	3.6	3.6
	Extensive	22	21
	Complete	65	30
Electric Substations	Slight	1	0.5
	Moderate	3	1.5
	Extensive	7	3.5
	Complete	30	15

4.3. Hydrogen Demand Scenarios

The hydrogen demand scenarios for 2050 are based on estimates that consider the use of this energy carrier for fertilizer and methanol production. The forecast for 2050 is presented in Table 4.8, based on the information presented by the authors of [106].

Two scenarios are then constructed based on the estimate of hydrogen demand for 2050: intermediate and concentrated, to contrast topologies. Table 4.9 displays the intermediate distribution of H2 demand, which is concentrated in the main cities of New Zealand: Auckland

(AKL), Taranaki (TRN), Wellington (WELL), Canterbury (CAN), and Otago (OTG). On the other hand, Table 4.10 indicates that all H2 demand is located in the Taranaki (TRN) region, which corresponds to the main port of New Zealand.

Table 4.8: Regional demand for hydrogen under the Distributed scenario.

Distributed H2 Demand Scenario		
Region	Annual Demand [Mt]	Hourly Demand [kt]
NIS	1.0	0.1
AKL	70	8.1
WTO	12	1.3
BOP	12	1.3
HBY	13	1.5
TRN	62	7.1
CEN	12	1.4
WEL	35	4.0
NEL	9.2	1.1
CAN	39	4.5
OTG	19	2.1
Total	284	36

Table 4.9: Regional demand for hydrogen under the Intermediate scenario.

Intermediate H2 Demand Scenario		
Region	Annual Demand [Mt]	Hourly Demand [kt]
AKL	84	9.5
TRN	86	9.8
WEL	48	5.5
CAN	48	5.5
OTG	19	2.2
Total	284	36

Table 4.10: Regional demand for hydrogen under the Concentrated scenario.

Concentrated H2 Demand Scenario		
Region	Annual Demand [Mt]	Hourly Demand [kt]
TRN	284	36

4.4. Scenarios Simulations

The present study will analyze 1,500 simulations corresponding to the generation of 500 earthquakes for each of the three hydrogen demand scenarios in New Zealand in 2050: distributed, intermediate, and concentrated. For each simulation case, 500 earthquakes will be generated throughout all regions of the model according to a uniform distribution of epicenters. Each event is simulated for 300 hours, commencing the simulation five hours before the occurrence of the earthquake.

Chapter 5

Results and Analysis

In this section, following the introduction of the connection approach between the resilience framework and REMix-NZ, an analysis of New Zealand's resilience for 2050 regarding H2 production is presented. Section 5.1 presents the New Zealand power system expansion for each hydrogen demand scenario. Then, section 5.2 discusses the results of integrating shut-down profiles related to natural disasters into REMix-NZ. Subsequently, Section 5.3 delves into examining earthquake resilience in New Zealand, while Section 5.4 compares earthquake responses based on the three hydrogen demand configurations.

5.1. New Zealand Power System Expansion for 2050

The results of the electric system expansion for each hydrogen demand scenario, obtained from the Solve Run, are presented in Figure 5.1.

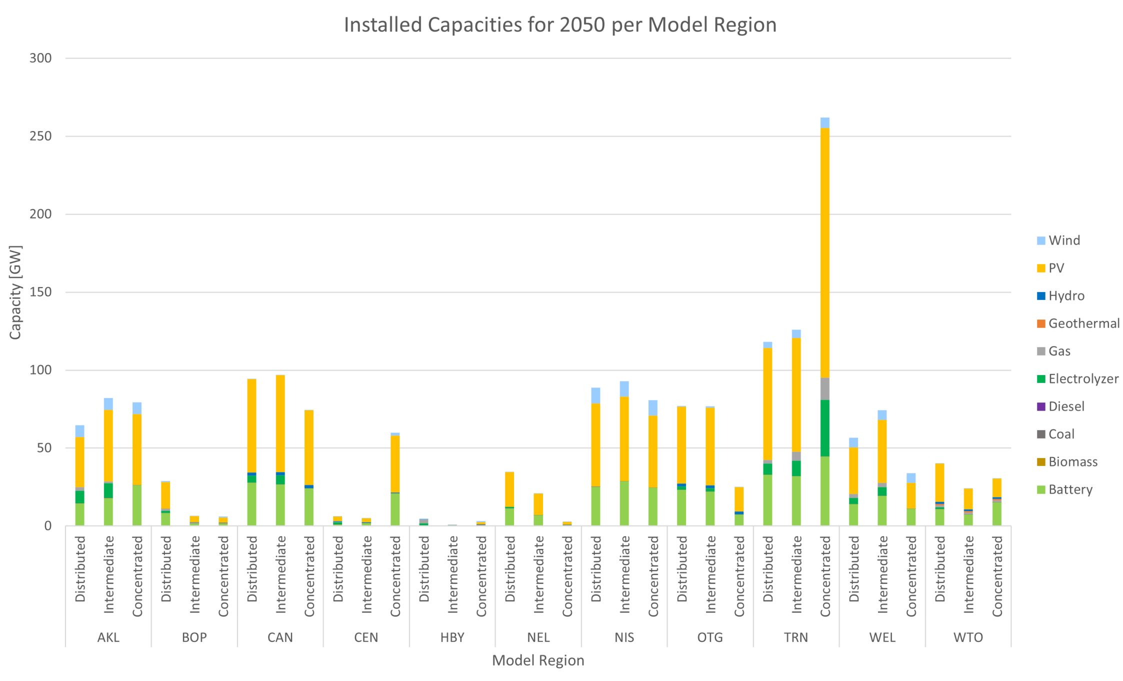

Figura 5.1: Installed capacities by technology in each hydrogen scenario for the year 2050 according to the New Zealand model region.

It can be observed that, first and foremost, each scenario exhibits a distinctive expansion trajectory contingent on its specific hydrogen demand. To satisfy the demand in each scenario, the expansion of capacity is primarily focused on solar technology and battery storage. Similarly, it can be observed that the expansion of technologies is responsive to the demand in each region. This is particularly evident in the Taranaki node, where all hydrogen demand is concentrated in the aforementioned scenario. This justifies the necessity of expanding the electricity system at that point in the aforementioned case.

Given that each hydrogen demand scenario entails a distinct network topology, the costs associated with the expansion and operation of each system will also vary. Table 5.1 presents the total costs associated with each scenario, which are obtained by summing the costs of unserved energy, fixed operation and maintenance costs, fuel costs, and investment costs for all technology units.

Table 5.1: Detail of New Zealand's electricity system costs under each hydrogen demand scenario.

Cost Indicator	H2 Demand Scenario		
	Concentrated	Intermediate	Distributed
Energy Not Served [MEUR]	0.11	0.14	0.15
OPEX Fix [MEUR]	228.96	137.16	135.77
Fuel Cost [MEUR]	1,198.21	852.59	868.43
CAPEX [MEUR]	18,557.40	16,324.30	16,320.20
Total Sistem Cost [MEUR]	19,984.68	17,314.19	17,324.55

A comprehensive examination of the total cost associated with each hydrogen demand scenario reveals that the concentrated hydrogen scenario represents the highest cost. This is largely attributed to the necessity for significant investment in enhanced generation and transmission capacity, a phenomenon that is elucidated in greater detail with respect to specific technologies in Figure 5.2.

The scenario of concentrated hydrogen demand implies a greater investment in generation infrastructure since it must prioritize the absorption of demand locally, particularly during peak demand hours in other regions. This results in the operation of transmission lines at their maximum capacity, preventing the absorption of hydrogen demand from being prioritized over electricity demand. Therefore, the concentrated demand scenario also implies an expansion of the transmission infrastructure. In contrast, the distributed and intermediate scenarios do not present significant differences in system expansion and cost.

The Annex B presents the investment costs associated with each technology and model region, classified according to the hydrogen demand scenario in question.

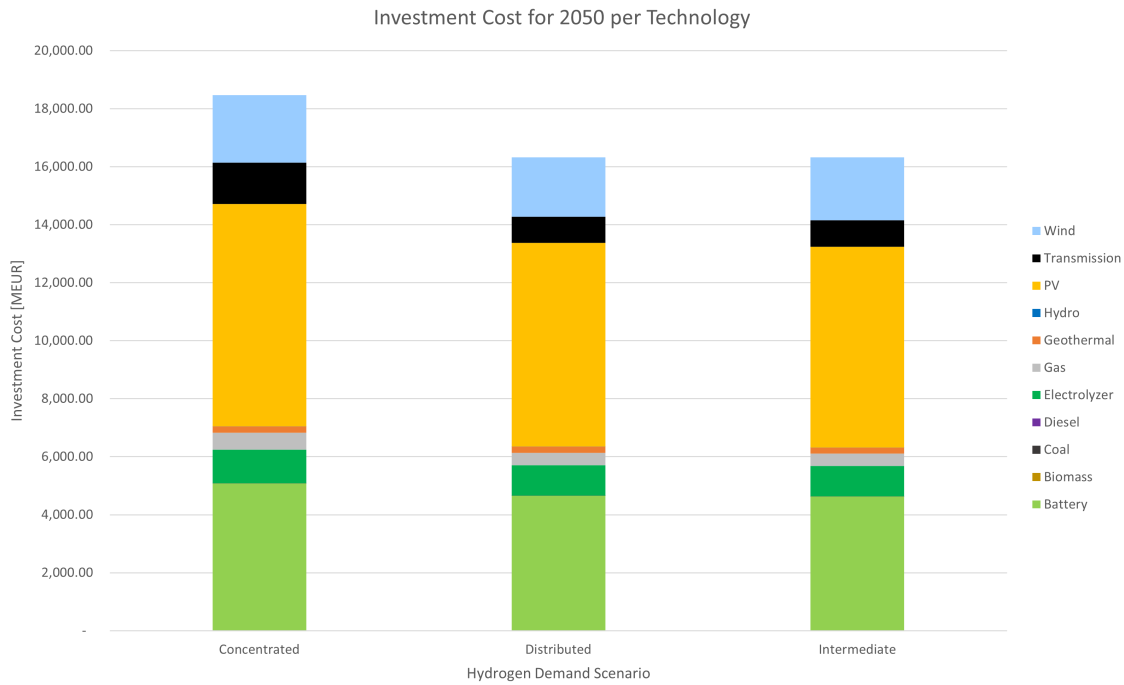

Figura 5.2: Investment cost by technology in each hydrogen scenario for the year 2050 according to the New Zealand model region.

5.2. Coupling of Resilience Assessment to REMix-NZ

Figure 5.3 demonstrates the successful integration of the resilience framework into REMix-NZ, exemplified by the scenario *Distributed Hydrogen Demand*. Figure 5.3.a illustrates the contrast between two separate runs. The *Solve Run* encompasses the initial system expansion and operation for 2050 to illustrate its behavior under normal conditions and the average electrical generation from 500 *Resilience Runs*. The aforementioned runs depict an earthquake-induced HILP event that causes a deviation from normal operation, as shown in Figure 5.3.b.

The average of the resilience runs reveals that system operations exhibit differences about five time-steps after optimization initiation, coinciding with earthquake occurrences. Subsequently, on average, the system undergoes significant discrepancies for approximately 100 hours before gradually converging toward stability. The distinctive spike near the end of this period signifies pronounced deviations between normal system operation and resilient run averages. This change could be attributable to original conditions such as reduced availability of renewable resources (specifically solar) or congestion in the HVDC link connecting islands.

The interpretation of Figure 5.3.b allows us to infer that it represents the average level of reorganization required by a disturbed system following an earthquake event. This indicator demonstrates that higher levels of requisite reorganization correspond to more significant resource deployment for contingency responses that were not considered in the operations with regular conditions. These results demonstrate that with REMix-NZ is it possible to identify the occurrence of a disruptive event and that it can effectively optimize an operation with generation and load disconnection profiles.

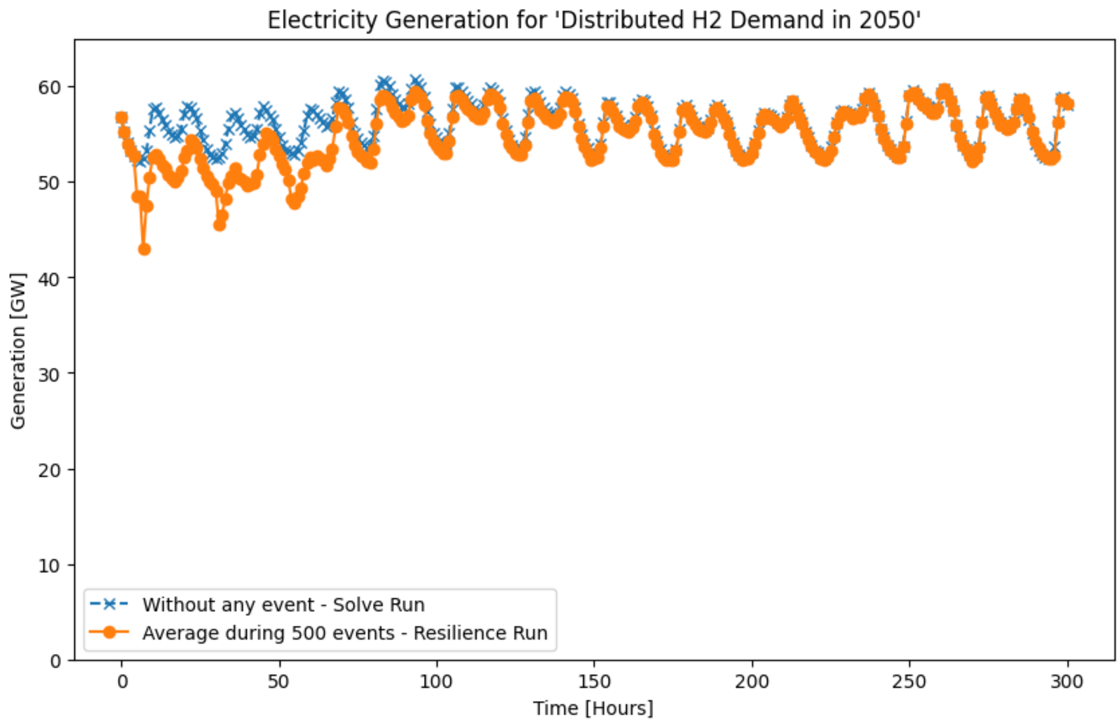

(a) Comparison of the electrical generation over time in the Solve Run and the average electrical generation for 500 events in the Resilience Run.

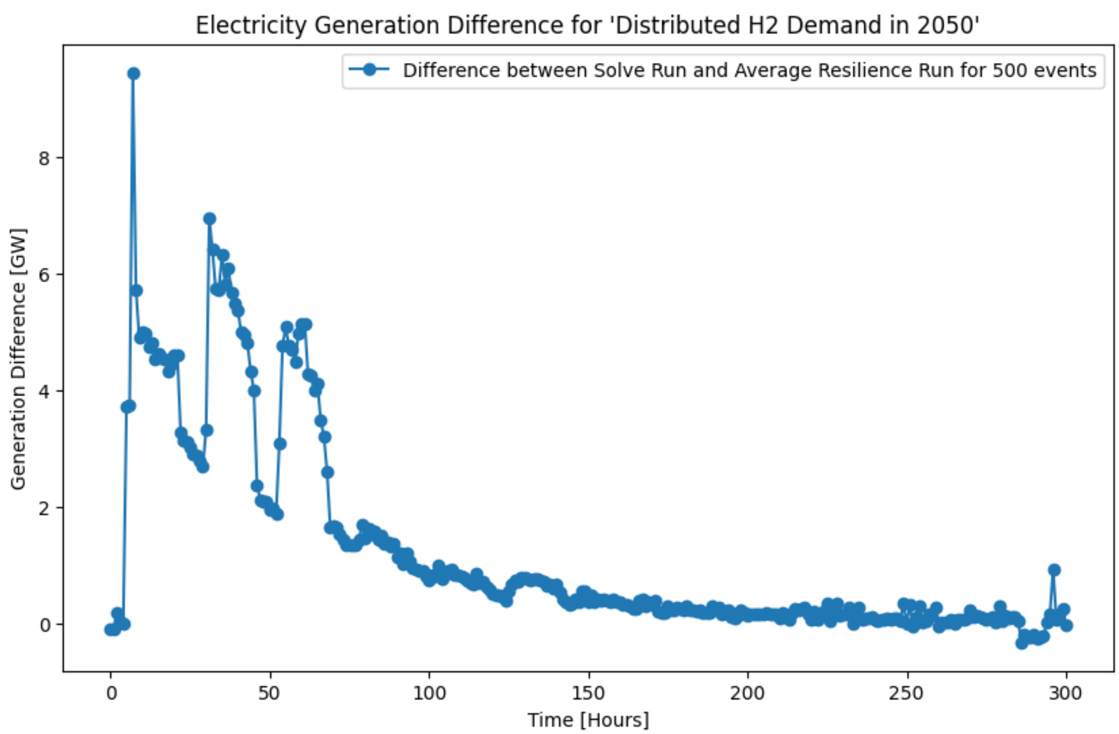

(b) Difference over time of the electrical generation between the Solve Run and the average of 500 Resilience Runs.

Figura 5.3: Coupling verification for REMix-NZ and the resilience framework using the "Distributed Hydrogen Demand" scenario.

5.3. New Zealand Power System Vulnerable to Earthquakes

It is evident that New Zealand is situated at the intersection of the Pacific and Australian tectonic plates, a fact that renders the occurrence of an earthquake a constant and unpredictable concern in the country. This is particularly pertinent in the context of the HILP event. Consequently, understanding the impact of this unanticipated event on the electrical system is essential for developing a resilient system capable of withstanding such an event.

Figure 5.4 illustrates the distribution of the capacity lost per technology when 500 events occur for the base case scenario with distributed hydrogen demand.

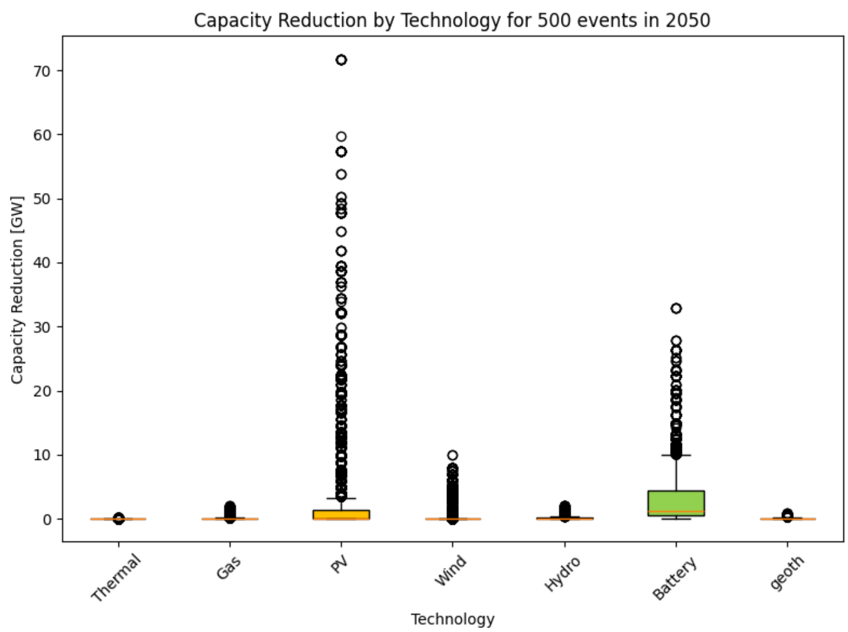

Figura 5.4: Box plot of the generation capacity reduction per technology resulting from 500 earthquakes in the "Distributed Hydrogen Demand" scenario.

The occurrence of an earthquake results in damage to all technologies, with the greatest impact concentrated below 5 MW, as illustrated at the top of each technology box. Nevertheless, isolated disconnections reach up to 70 GW in isolated cases, particularly for photovoltaic (PV) and batteries, the most installed capacities in the system. This is substantiated by fragility curves and a high peak ground acceleration (PGA) calculation, which increases the probability of a more catastrophic damage state. Moreover, the most extreme cases can be attributed to the fact that in REMix-NZ, the representative system of New Zealand nodal, i.e., all regional generation classified by technology, is connected to the system at a single point, which corresponds to the epicenters selected to simulate the set of earthquakes.

The recovery of the various sectors of the system, which respond to the recovery curves of generation units and high-voltage electrical substations, is illustrated in Figure 5.5.

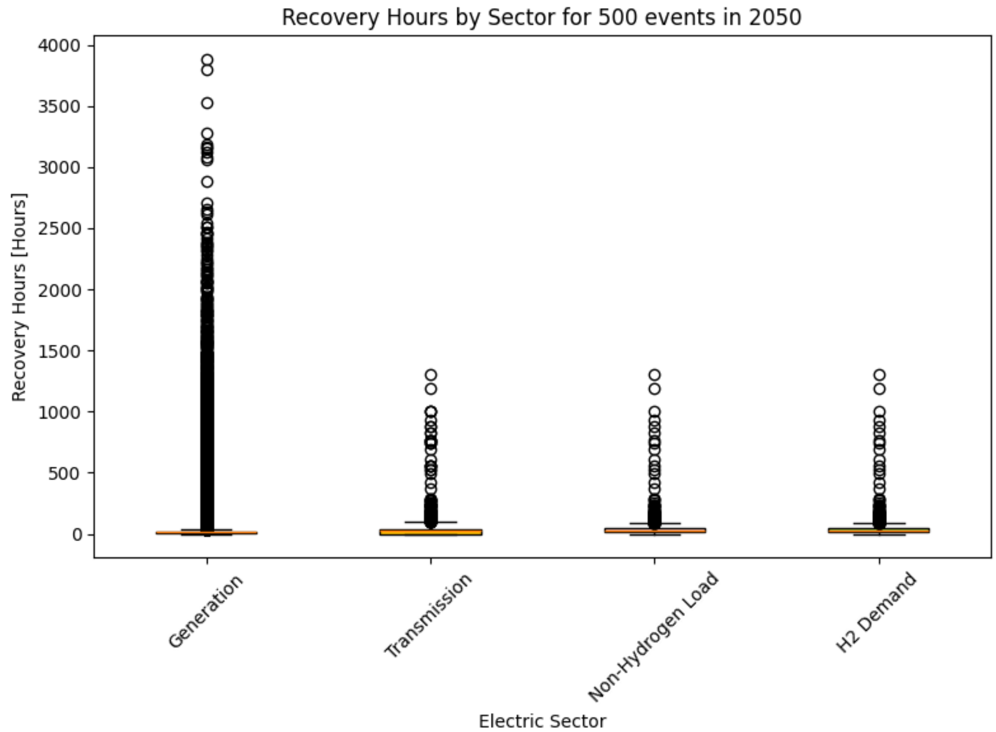

Figura 5.5: Box plot of the hours of recovery of 100 % of the operating capacity of each electrical sector resulting from 500 earthquakes in the “Distributed Hydrogen Demand” scenario.

The restoration of the electric sector is concentrated in the initial 125 hours following the earthquake, with 75 % of the restoration occurring within this period. It is noteworthy that the recovery of transmission capacity allows for the reconnection of lost demand, including non-hydrogen load and hydrogen demand, in the event of HILP occurrences. The restoration process in the generation sector is observed to occur over a greater time interval, with some generation units requiring almost 3,500 hours to resume normal operations. This is based on the standard deviation of the normal distribution of the recovery in the complete damage state, as presented in Table 4.7. It can be inferred that 99.9 % of the restoration occurs within the three standard deviation interval.

The damage to the connected non-hydrogen load is proportional to the percentage of damage in its connection node. Similarly, the transmission system damage is proportional to the same logic. However, the graph presented in Figure 5.5 indicates that the damage is more significant in this case, as a node can be connected to several lines. Consequently, when an earthquake damages a node, the capacity of all the connected transmission facilities is reduced as well as the non-hydrogen and hydrogen demand.

The New Zealand electricity system planning and expansion for the year 2050 indicates that the occurrence of a HILP event, particularly an earthquake, will inevitably result in damage to the components of the electricity system. This damage is probabilistically inevitable. Consequently, integrating hydrogen as a new supply-demand implies expanding the system. Based on this new addition, a new large demand must be provided. Thus, the available resources must be exploited according to increased solar generation and storage capacity projection.

The integration of hydrogen for the year 2050 is not a topic of discussion. Therefore, the real discussion is what the strategic distribution of the network should be to respond more effectively to an event whose damage is inevitable. However, its study allows for the implementation of preventive planning measures to reduce damage to infrastructure and energy not served as a result of damage to systemic components that allow for the supply of demand.

5.4. Distributed Hydrogen Improves Resiliency

5.4.1. Resilience Metrics

Tables 5.2 and 5.3 present the mean and *condition value at risk* (CVaR of 5 % worst cases) resilience metrics obtained for generation and non-hydrogen load, respectively. The non-hydrogen load includes the average and CVaR of the load not served.

Table 5.2: Resilience metrics calculated for the Generation Availability curve by simulating 500 events in each hydrogen demand scenario.

Generation Availability						
Resilience Metric	Concentrated		Intermediate		Distributed	
	Mean	CVaR	Mean	CVaR	Mean	CVaR
F	-	-	-	-	-	-
L [%]	26	64	19	44	18	42
E [hrs]	41	285	60	287	39	271
P [GW restored/h]	0,026	0,063	0,019	0,066	0,023	0,211

Table 5.3: Resilience metrics calculated for the Non-Hydrogen Load curve by simulating 500 events in each hydrogen demand scenario.

Non-Hydrogen Load						
Resilience Metric	Concentrated		Intermediate		Distributed	
	Mean	CVaR	Mean	CVaR	Mean	CVaR
F	-	-	-	-	-	-
L [%]	6	20	6	19	6	18
E [hrs]	33	197	39	218	35	175
P [GW restored/h]	0,042	0,042	0,045	0,053	0,044	0,034
Non-Hydrogen Load Not Served [GWh]	47,720	50,240	51,320	54,020	47,700	50,220

Figure 5.6 depicts the average and CVaR FLEP resilience metrics for the three hydrogen demand scenarios based on an average of 500 earthquake occurrences. These metrics enable the assessment of resilience in relation to operations, specifically concerning generation capacity and non-hydrogen load disconnection during events.

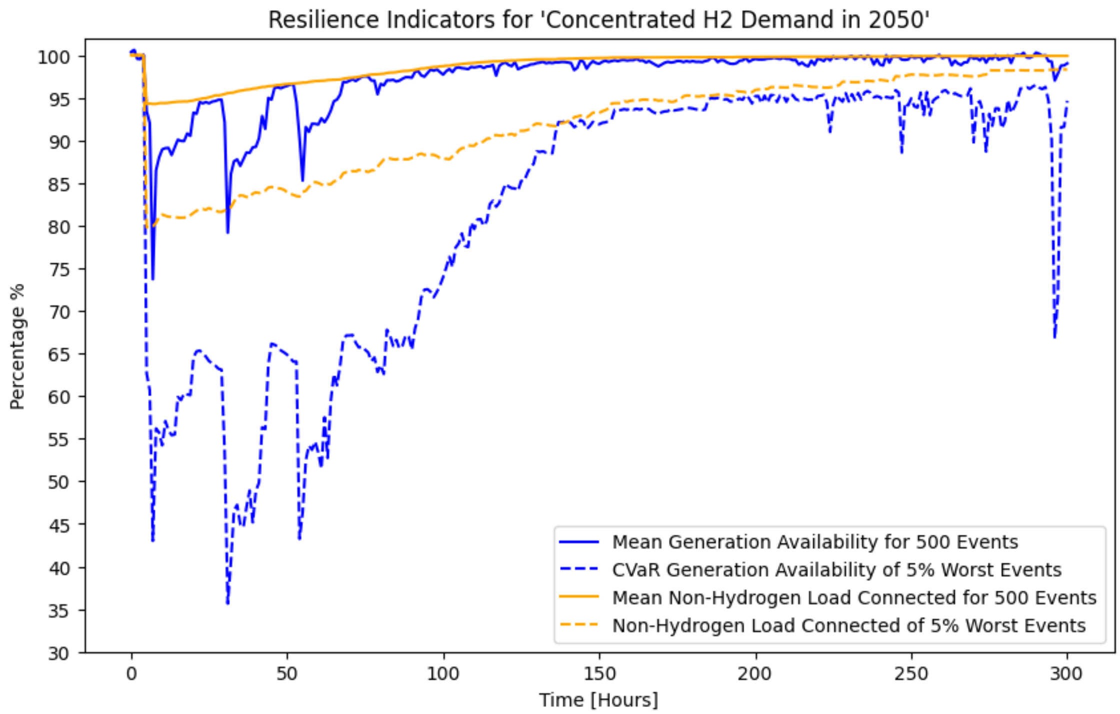

(a) Concentrated Hydrogen Demand scenario.

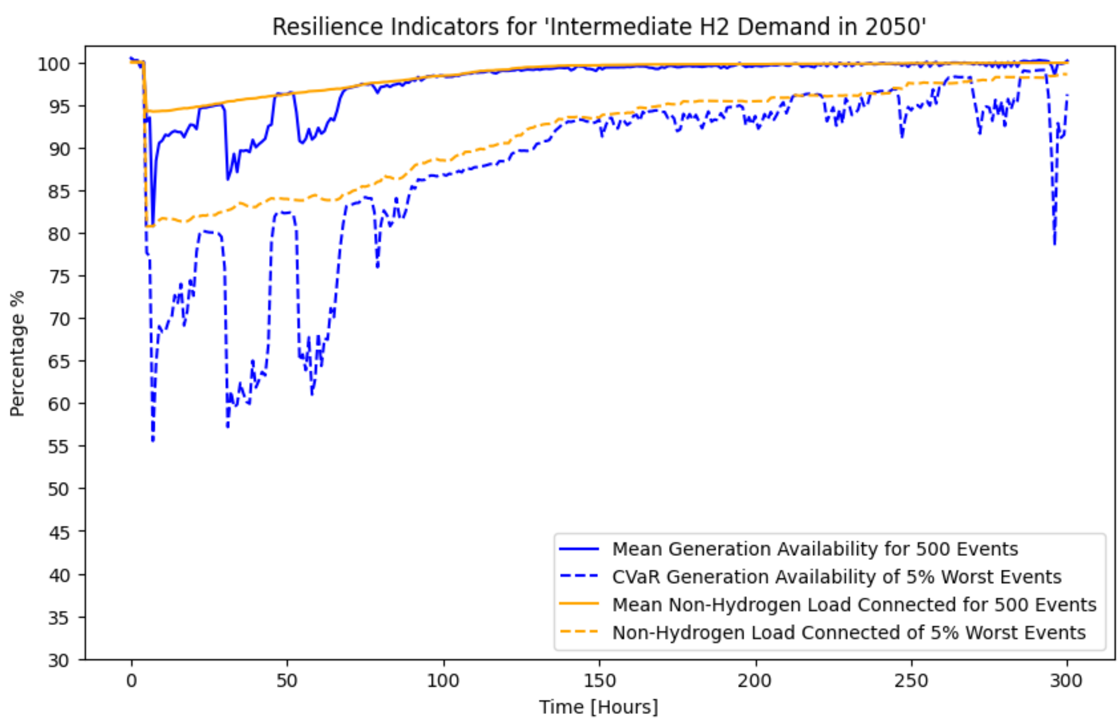

(b) Intermediate Hydrogen Demand scenario.

Figura 5.6: Average percentage of installed generation and load capacity over time for each hydrogen demand scenario.

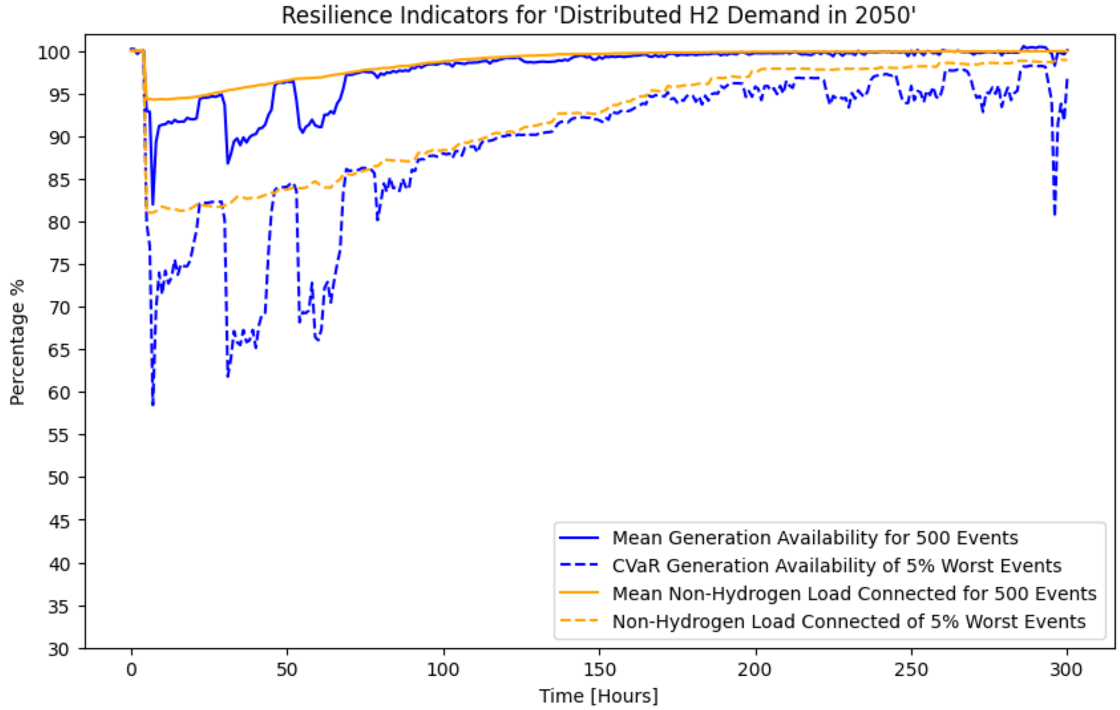

(c) Distributed Hydrogen Demand scenario.

Figura 5.6: Average percentage of installed generation and load capacity over time for each hydrogen demand scenario (cont).

About the average LEP metrics for generation, illustrated in Table 5.2 and Figure 5.6, it can be observed that irrespective of the hydrogen demand scenario, the deterioration of generation operations is more pronounced than the operational deterioration of non-hydrogen demand. This is justified by the loss of non-hydrogen load caused exclusively by damage at the connection point -namely the transmission node-. It is important to note that damage at the transmission node reduces the capacity for all elements connected, including the generation. The more intense damage experienced by the generation sector, which could be called “double damage”, occurs due to two distinct causes: the fragility curves and the PGA determine the damage to the generation facilities, and the damage to the connection point between the grid and the generation facilities further exacerbates the situation.

A deeper examination of the resilience metrics obtained for generation availability reveals that the systems exhibit a distinct topology, a direct consequence of modifying the distribution of hydrogen demand within the system. Consequently, the mean and CVaR values indicate that a distributed positioning of hydrogen demand results in a more resilient expansion of the system, as evidenced by its superior performance in terms of FLEP metrics compared to other scenarios.

The results of the average calculations indicate that the more resilient hydrogen demand scenario is distributed, whereas the less resilient concentrated spatial placement is based on a lower initial drop and a less prompt recovery. Conversely, an examination of the resilience metrics for the 5 % most adverse scenarios reveals that the distributed hydrogen demand exhibits superior performance in terms of a less pronounced drop, a more expedient resumption of generation, and a shorter duration of the damage stage. Nevertheless, it is noteworthy that in the most adverse cases, a complete recovery is not achieved within the 300-hour optimization period.

The average non-hydrogen load's resilience to earthquakes presents a similar behavior in all hydrogen demand scenarios. It is understood that the damage to the demand comes from the damage and subsequent re-connection of the node to which it is connected. This corresponds to an output of the resilience framework introduced as input to REMix-NZ.

Upon examination of the anticipated performance of the 5 % most unfavorable cases, it can be observed that the distributed scenario exhibits a marginal improvement in terms of load resilience.

Upon closer examination of each resilience metric, specifically metric L, as illustrated in Figure 5.6.a, it can be observed that the highest average and CVaR generation and non-hydrogen degradation correspond to the concentrated demand scenario. This is due to the location of the epicenter of the simulated earthquakes, which justifies this result. This is due to the fact that in the case of concentrated demand, earthquakes with epicenter in the North Island, where the hydrogen demand is located and where the generation facilities—particularly solar—that supply this demand are concentrated, are more devastating. This justifies the possible untimely disconnection and therefore the more pronounced initial drop.

Metric E, which reflects the extent of system degradation in the event of earthquakes, indicates that the most favorable scenario from the generation perspective corresponds to the distributed hydrogen demand, in contrast to the worst-case scenario, which is related to the intermediate hydrogen scenario. This can be justified by the repercussions of the damage experienced by the generation sector in both scenarios. Consequently, given that the expansion of each scenario was conducted independently in accordance with their respective characteristics, a greater concentration of demand resulted in a greater expansion of the generation capacity located in proximity to these centers of hydrogen consumption. Consequently, a greater amount of capacity remains disconnected for a longer period and its reconnection is slower due to the larger "blocks" involved.

Finally, with regard to the speed of system recovery, P, the lowest variation per unit of time and, therefore, the slowest average recovery is observed in the intermediate scenario. The calculation of this metric is conducted from a level of 96 % of the connected generation capacity to 100 %, thus negating the disadvantage previously observed for the intermediate scenario in terms of the extension of the damage state. Instead, it can be seen that the generation blocks, corresponding to nodal generation by reconnected technology, recover faster in this section, which is now understood to be a benefit.

In the event of a disruption to the power supply, it is observed that the reconnection of generation is much faster in the case of distributed demand. This is because, although no scenario experiences 100 % connection, the generation is also slightly distributed.

The final metric presented in Table 5.3 corresponds to the non-hydrogen load not served, which is illustrated graphically for each scenario in the histograms in Figure 5.7.

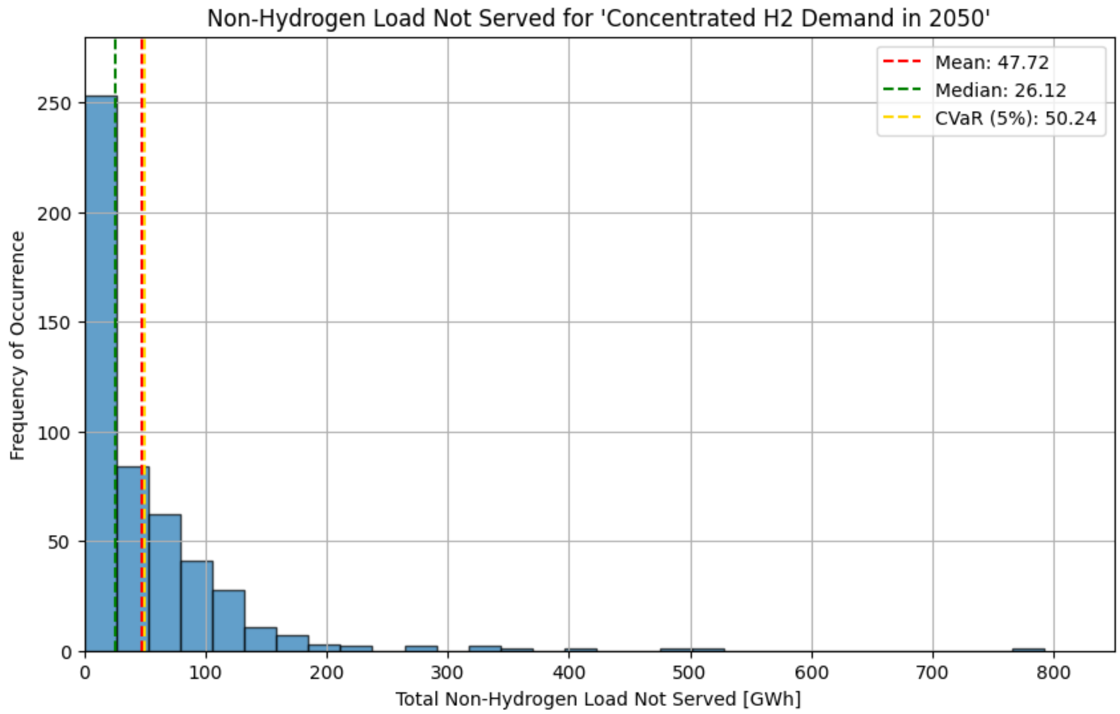

(a) Concentrated Hydrogen Demand scenario.

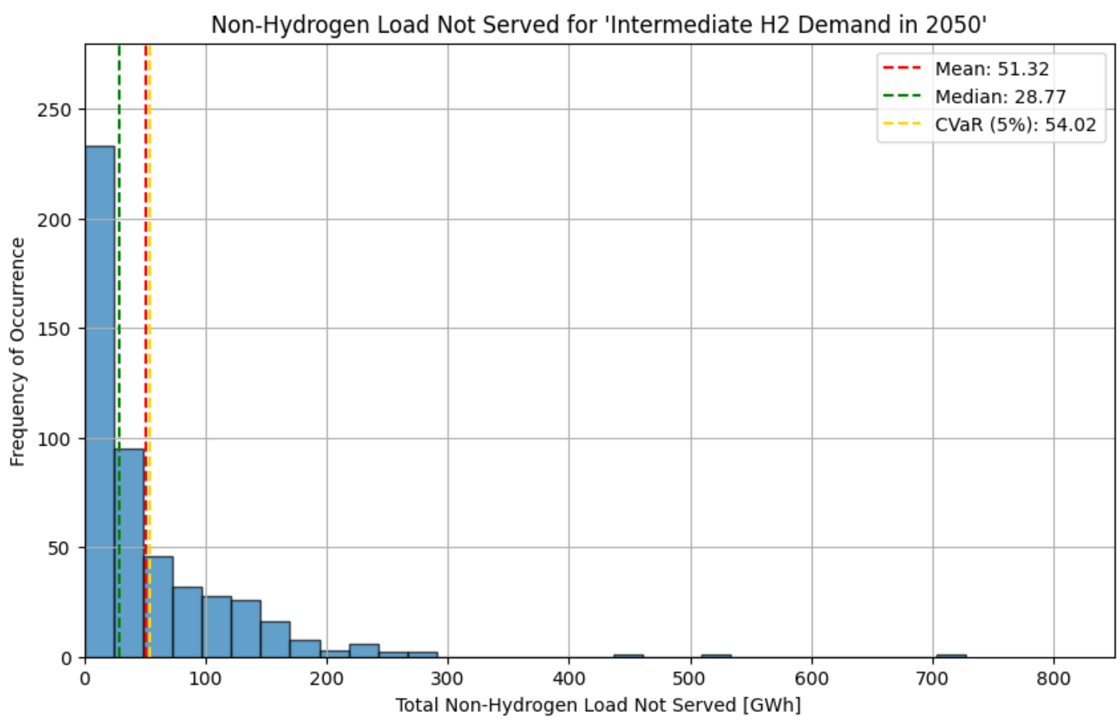

(b) Intermediate Hydrogen Demand scenario.

Figura 5.7: Histogram of the Energy Not Served for 500 events simulated in each hydrogen demand scenario presenting mean, median, and CVaR metrics.

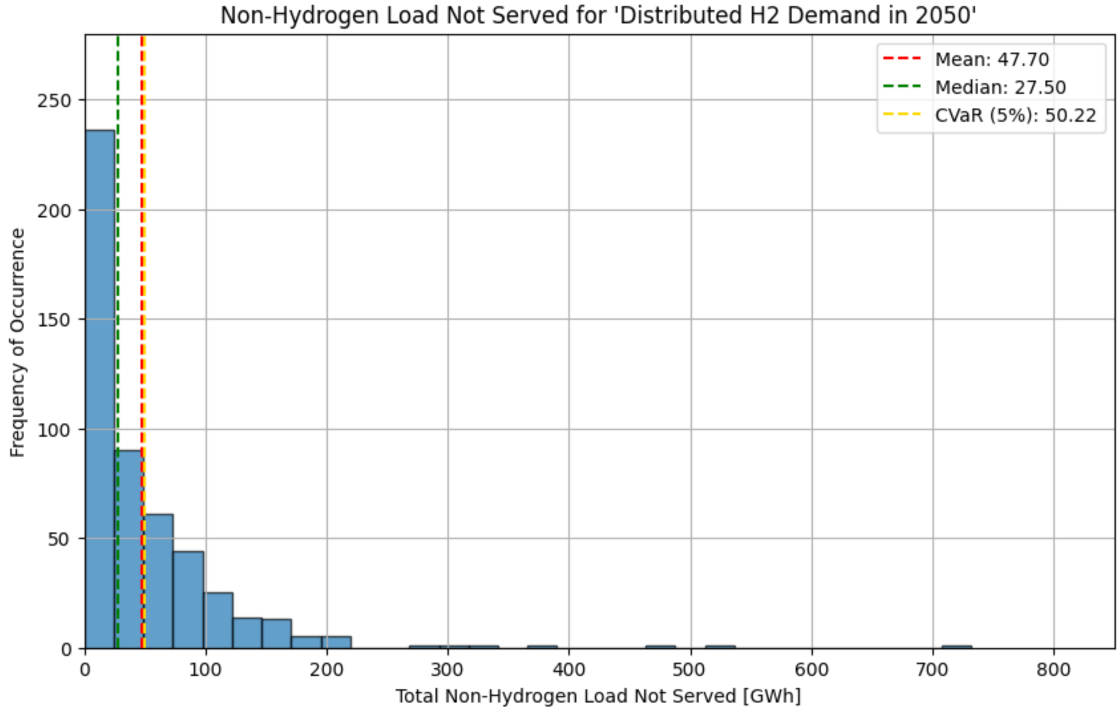

(c) Distributed Hydrogen Demand scenario.

Figura 5.7: Histogram of the Energy Not Served for 500 events simulated in each hydrogen demand scenario presenting mean, median, and CVaR metrics (cont).

As previously stated, the not-served non-hydrogen load is a direct consequence of the disconnected demand due to damage at the connection node. Consequently, this corresponds to an output of the resilience framework and an input to REMix-NZ. Therefore, there are no significant differences between the hydrogen demand scenarios. From a load resilience perspective, the superiority or inferiority of a scenario is very subtle.

5.4.2. Energy Not Served Performance

Figure 5.8 presents each hydrogen demand scenario's non-hydrogen load not served. This corresponds to the electricity purchased and sold without considering the demand associated with the operation of the electrolyzer. Figure 5.8.a presents the behavior of this variable over time. Figure 5.8.b is the unserved load as a percentage of the total non-hydrogen demand. Figure 5.8.c presents the behavior of the non-hydrogen load not served over time of the 5 % worst cases.

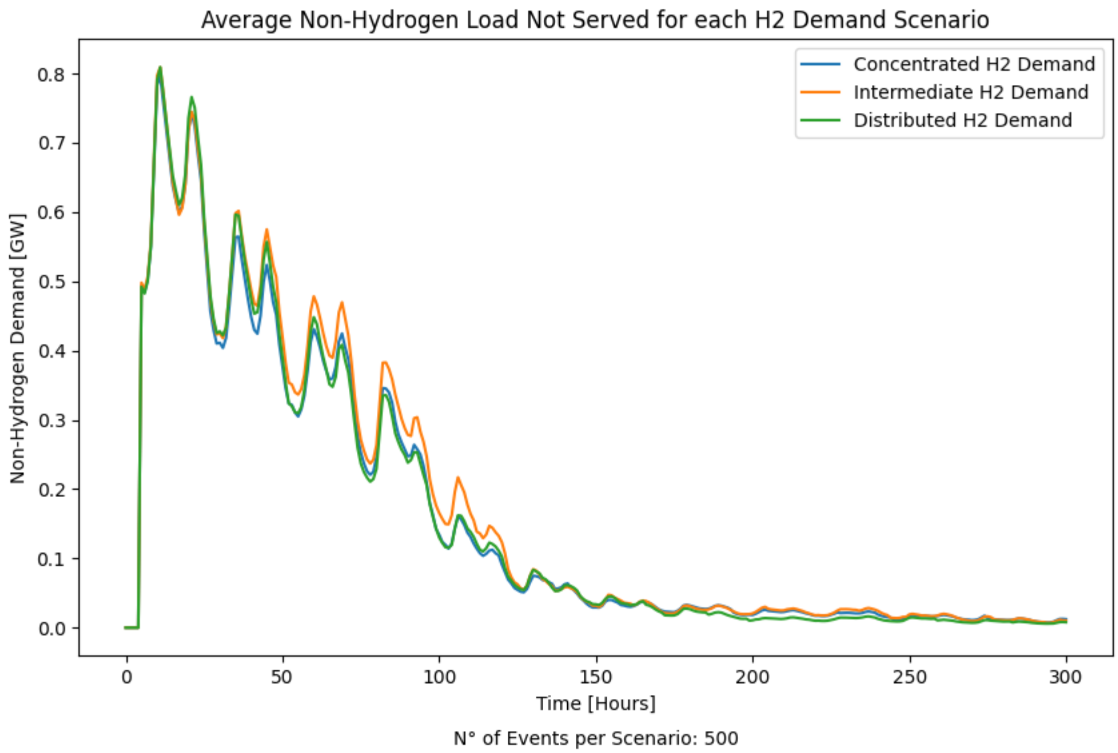

(a) Comparison of the average Non-Hydrogen Load Not Served over time of 500 events (Resilience Runs).

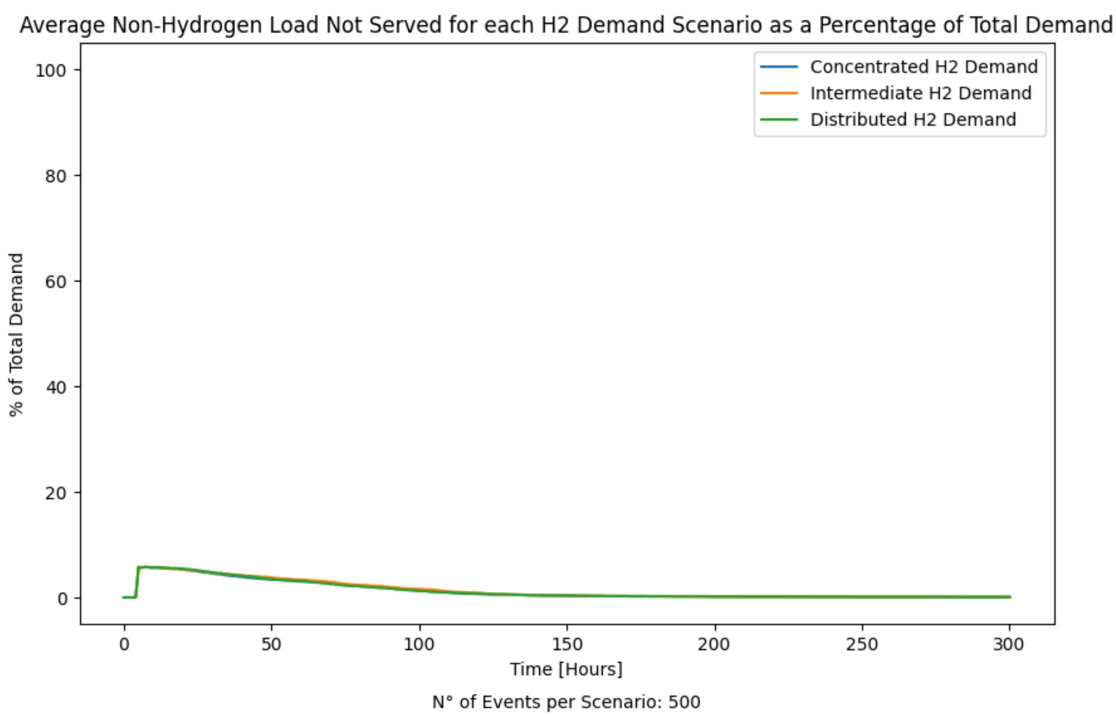

(b) Comparison of the average Load Not Served of 500 events (Resilience Runs), ordered from highest to lowest.

Figura 5.8: Non-Hydrogen Load Not Served comparison of the hydrogen demand scenarios.

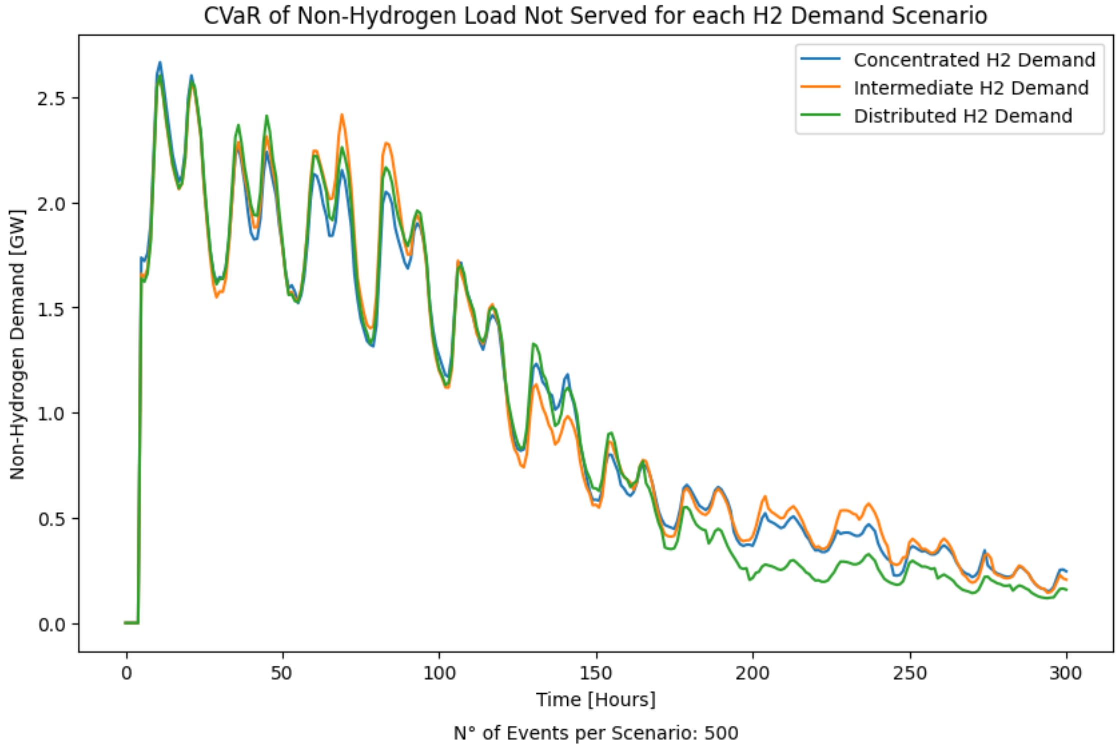

(c) Comparison of the CVaR Non-Hydrogen Load Not Served over time of 500 events (Resilience Runs).

Figura 5.8: Non-Hydrogen Load Not Served comparison of the hydrogen demand scenarios (cont).

As evidenced by the resilience metrics previously analyzed, the non-hydrogen load not served plots demonstrate that no scenario can be identified as superior or inferior in performance. This is substantiated by the fact that the non-served load is exclusively attributable to the damage of system nodes and the inability to supply demand due to a lack of transmission capacity. The proportion of damage to a system node is inversely proportional to the capacity of all components connected to that point.

The comparison of hydrogen not-served for each study scenario is presented in Figure 5.9. As with unsupplied demand, Figure 5.9.a presents the average unserved hydrogen over time, as a percentage of the total hydrogen demand 5.9.b. Finally, Figure 5.9.c illustrates the behavior of the worst-case 5 %.

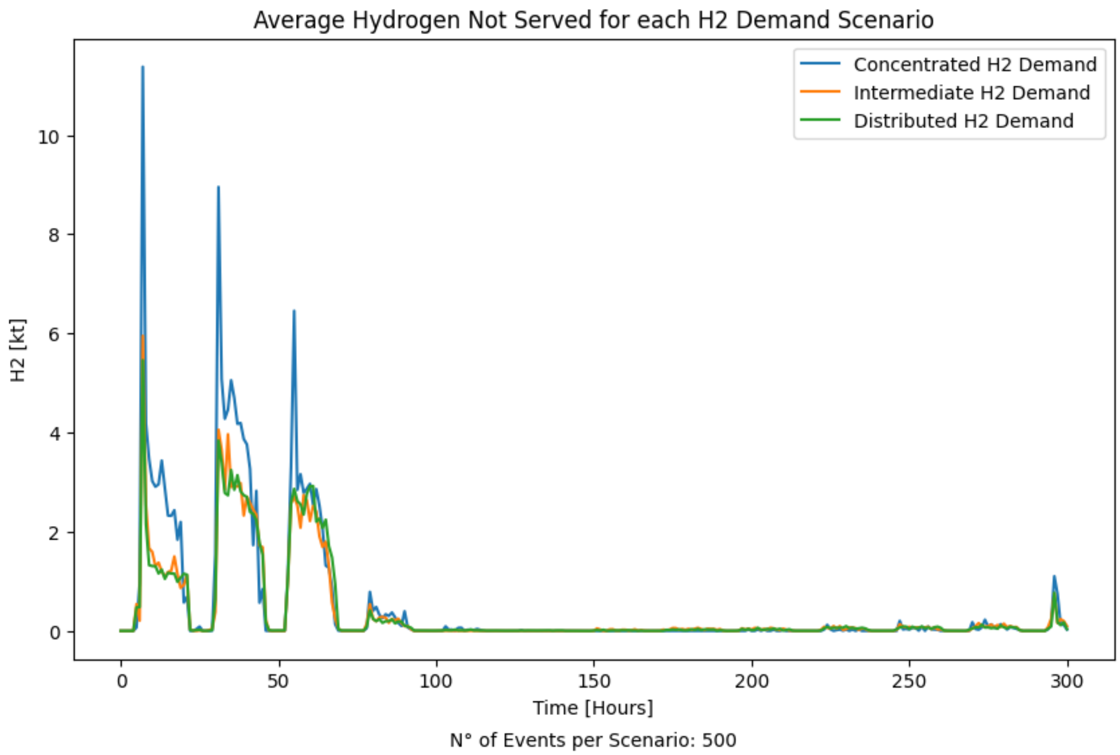

(a) Comparison of the average Hydrogen Not Served over time of 500 events (Resilience Runs).

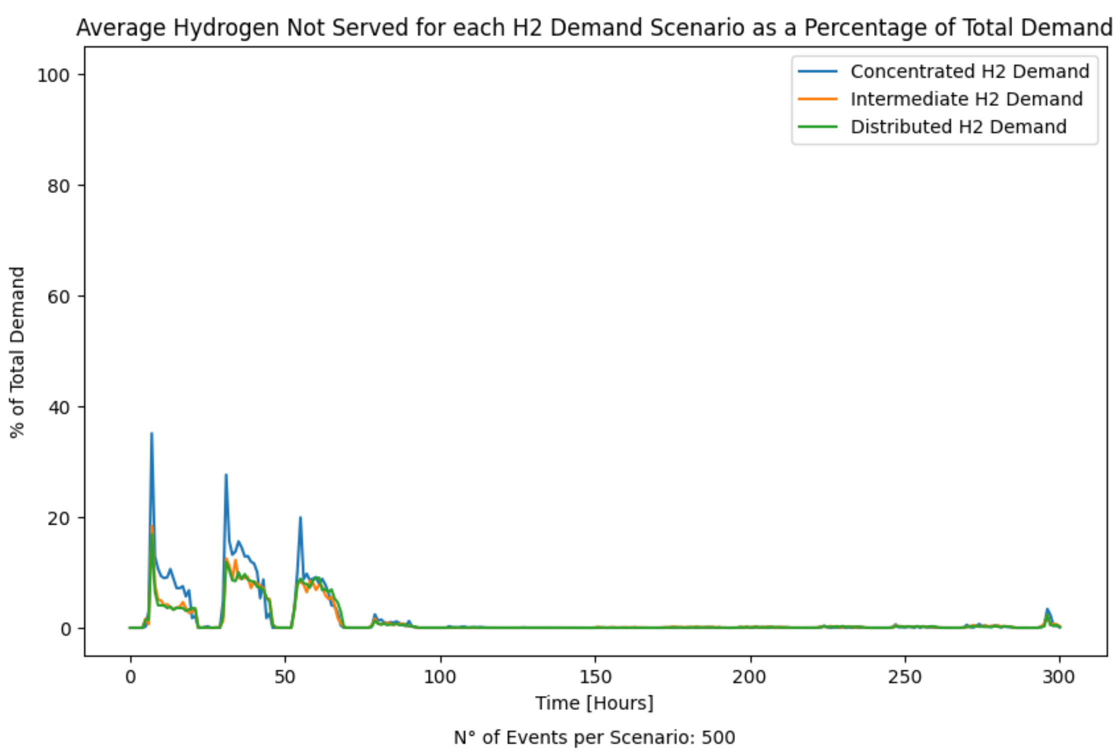

(b) Comparison of the average Hydrogen Not Served of 500 events (Resilience Runs), presented as a percentage of the total hourly demand.

Figura 5.9: Hydrogen Not Served comparison of the hydrogen demand scenarios.

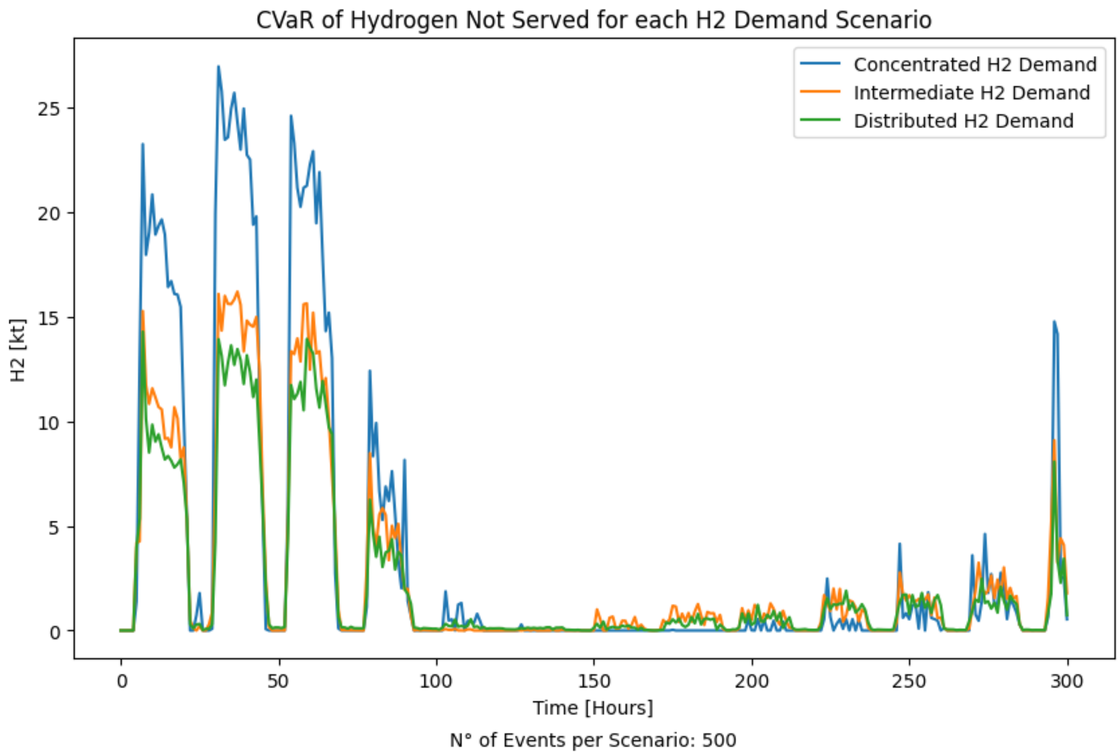

(c) Comparison of the CVaR Hydrogen Not Served over time of 500 events (Resilience Runs).

Figura 5.9: Hydrogen Not Served comparison of the hydrogen demand scenarios (cont).

Upon closer examination of the hydrogen not served, it becomes evident that the concentrated scenario corresponds to the one with the greatest “sacrifice” of hydrogen demand. This is substantiated by the fact that this scenario is subjected to the most detrimental set of events from the hydrogen perspective: the occurrence of the earthquake on the North Island, where the concentrated hydrogen demand is located. Given the flexibility of the system and the low hydrogen slack cost, the optimal response to the occurrence of earthquakes in the aforementioned zone is to sacrifice demand to ensure that the system continues to supply electricity, which has a higher penalty. This can also be understood to mean that the concentrated system configuration has fewer degrees of freedom to respond post-contingency.

In addition to the significant disruption to the hydrogen supply chain resulting from the earthquake on the North Island, the concentrated scenario is also significantly impacted by the earthquake on the South Island. This is because an earthquake in the south implies that the system must continue to supply a very large demand concentrated in the north, despite the fact that fewer resources are available and the interconnection between islands is stressed. In the most extreme cases, this hydrogen demand is not supplied, as shown in the CVaR metric in Figure 5.9.c.

5.4.3. Hydrogen Demand Performance

To further elucidate the analysis of hydrogen demand presented previously, Figure 5.10 is presented, which contrasts the hydrogen demand not served over time for each hydrogen scenario.

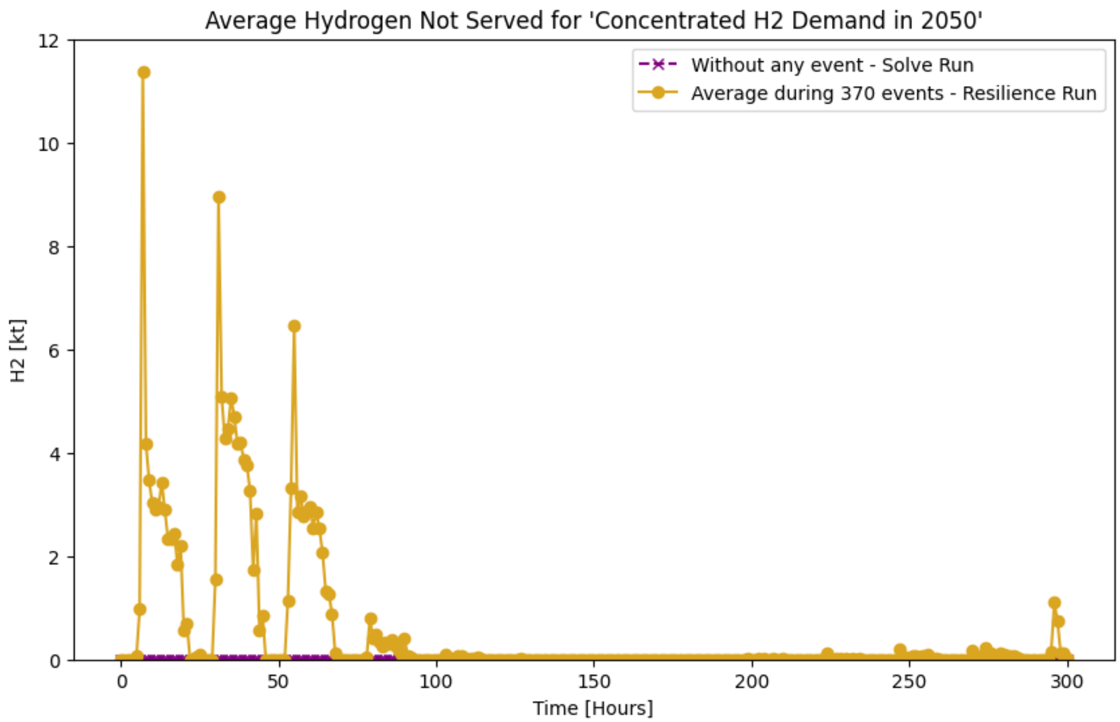

(a) Concentrated Hydrogen Demand scenario.

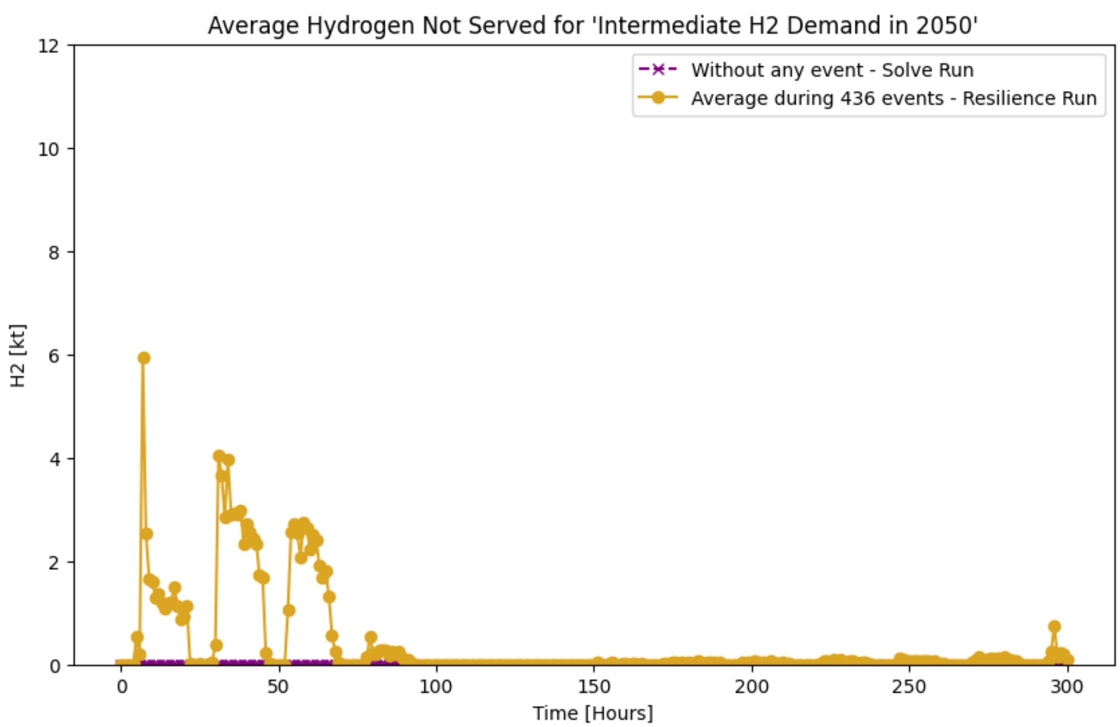

(b) Intermediate Hydrogen Demand scenario.

Figura 5.10: Comparison of Hydrogen Not Served over time between Solve Run and the average of 500 events (Resilience Runs).

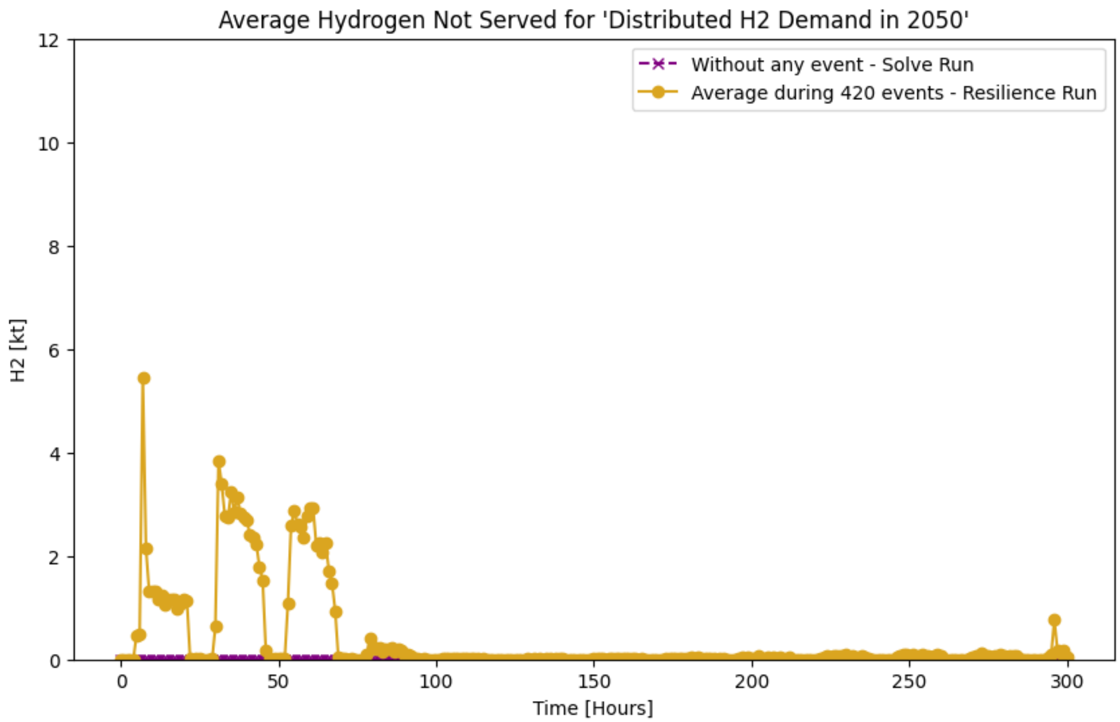

(c) Distributed Hydrogen Demand scenario.

Figura 5.10: Comparison of Hydrogen Not Served over time between Solve Run and the average of 500 events (Resilience Runs) (cont).

The results obtained indicate that not all simulated events produce energy not served. This is due to the direct impact of the epicenter of the earthquake and the distribution of hydrogen demand on the determination of whether hydrogen should be "sacrificed" to prioritize the supply of electricity demand rather than electrolyzer demand. Figure 5.10.a illustrates that the concentrated scenario exhibits the lowest number of unserved energy events. However, these events are more detrimental in light of the demand concentration in a region that may differ from the earthquake's epicenter. This makes it challenging to supply the demand in its entirety.

The previous analysis of unserved hydrogen revealed that it is less prevalent in the case of distributed hydrogen compared to intermediate hydrogen and that it is also experienced in fewer events. This is an intriguing finding, as distributed hydrogen represents a greater degree of freedom to respond to contingencies. However, its sacrifice is less necessary for the system to experience a better response to earthquakes, which allows us to conclude that this scenario has superior infrastructure and load resilience.

The histograms in Figure 5.11 show the frequency of the hydrogen demand not served for each simulated scenario. The mean, median, and CVaR of 5 % are presented for each scenario. The CVaR represents an arithmetic measure of the expected amount of loss in the worst 5 % of possible scenarios. A lower CVaR implies that the unserved hydrogen demand has a shorter tail towards the negative side, indicating that the respective scenario is less likely to experience very large losses.

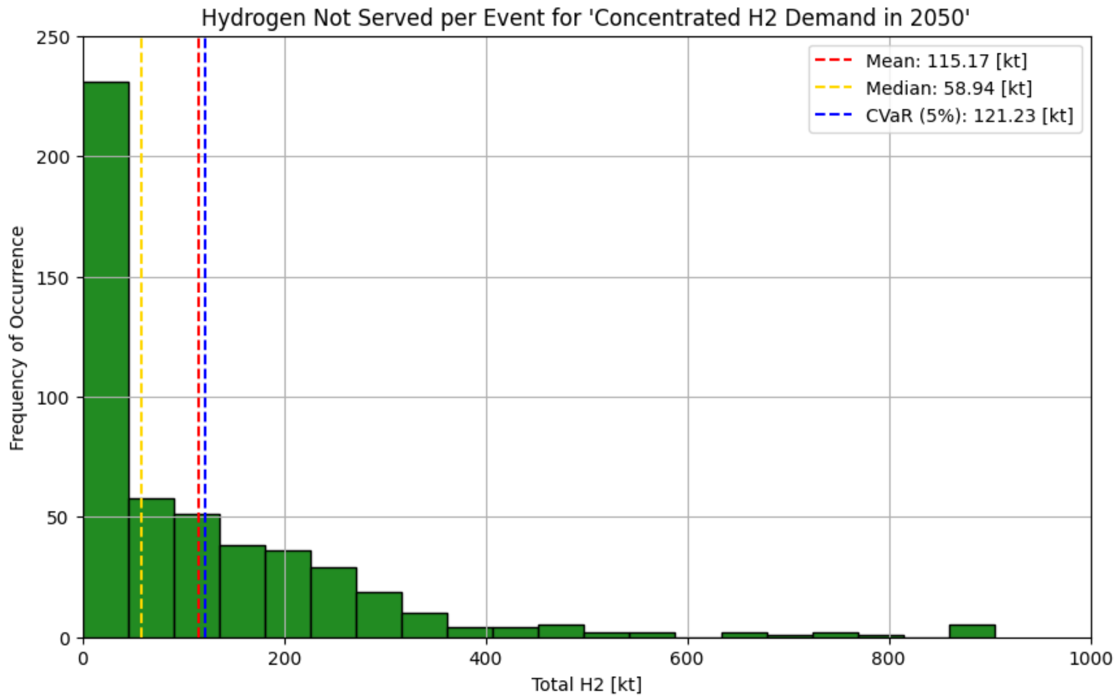

(a) Concentrated Hydrogen Demand scenario.

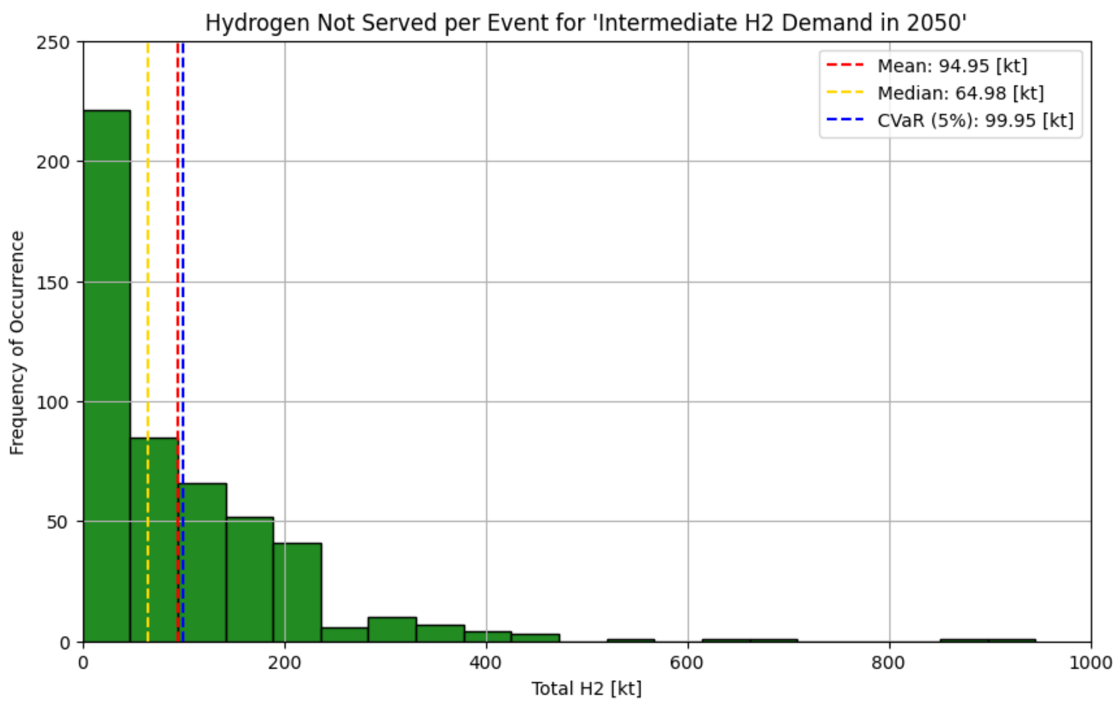

(b) Intermediate Hydrogen Demand scenario.

Figura 5.11: Histogram of the Hydrogen Not Served for each hydrogen demand scenario presenting mean, median, and CVaR metrics.

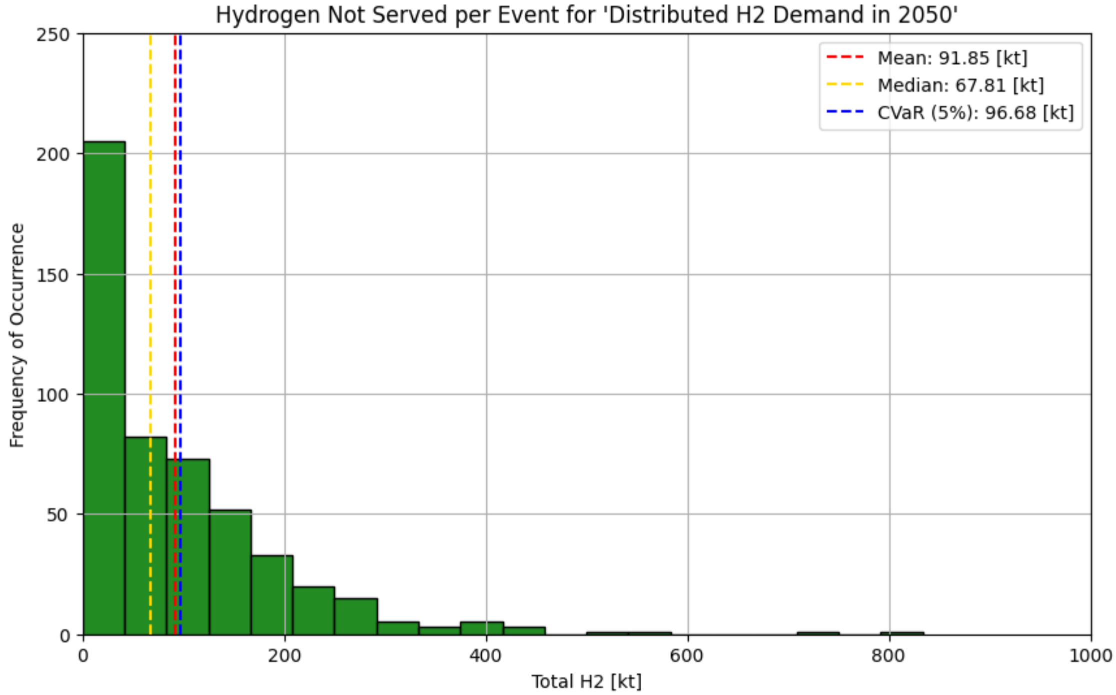

(c) Distributed H2 Demand scenario.

Figura 5.11: Histogram of the Hydrogen Not Served for each hydrogen demand scenario presenting mean, median, and CVaR metrics (cont).

From the CVar metrics of the analyzed scenarios, it can be observed in Figure 5.11.c that the “safest” scenario corresponds to the distributed hydrogen demand, as evidenced by the fact that on average, the unserved hydrogen demand does not show large deviations. This is not the case for the concentrated scenario, as evidenced by Figure 5.11.a, which shows a concentration of data in low amounts of hydrogen not served. While the concentrated scenario exhibits the most pronounced consequences, the intermediate case does not exhibit a discernible pattern of superior or inferior performance. This observation justifies the conclusion that these scenarios are not conducive to the expansion of the electricity system on average.

Chapter 6

Conclusions

The objective of this study was to evaluate the feasibility of different hydrogen demand scenarios to improve the resilience of the New Zealand electricity system in 2050 during seismic events. To develop this analysis, a framework capable of performing a resilience study was first constructed by introducing disconnection profiles associated with the occurrence of an untimely devastating event. Then, developing the optimization tool allowed for questioning the physical and operational consequences and damages that an earthquake can cause in an electrical system. Finally, the question of the most resilient hydrogen demand configuration was raised, given that the massive integration of this technology is necessary for the energy transition and that the occurrence of a disruptive event such as an earthquake is unpredictable and unavoidable.

The execution of thousands of simulations demonstrated the successful coupling of the resilience framework to the energy system optimization tool REMiz - NZ. The optimization of the operation of the electrical system after the occurrence of an earthquake that caused damage to the generation capacity and grid connection nodes evidenced a difference between the normal operation of the system (referred to as the “Solve Run” in the study) and the average of the runs with seismic events (referred to as the “Resilience Runs” in the study).

In the specific case of earthquakes occurring in a country with high seismic activity, such as New Zealand, it was observed that the electrical system planned for 2050 would inevitably be affected by the occurrence of a seismic event, affecting all the available generation technologies of the system and damaging the nodes of the system. This leads to questioning the poorly meshed topology of the representative scheme of the electrical grid. The national grid is particularly dependent on the interconnection between islands, which presents a significant challenge, particularly in light of the expected concentration of electricity demand in the northern island of the country, while generation is concentrated in the southern island. Furthermore, the estimation of the behavior of the electrical system, derived from fragility curves and recovery curves, underscores the significance of resilient planning, particularly the capacity to prepare the network in anticipation of the inevitability of HILP events.

In light of the objectives of the energy transition regarding the integration of hydrogen into energy systems, particularly the New Zealand grid, it is imperative to plan its addition to the grid in a reliable and resilient manner in the event of a high-impact seismic event. Thus, when comparing the arrangement of the scenarios in the grid between distributed, intermediate, and concentrated, the most resilient response was observed in the distributed scenario. Multiple justifications, including the metrics of FLEP, non-hydrogen load, and unserved hydrogen, evidence this. Statistical metrics such as the median, mean, and CVar were employed to support this conclusion. A clear contrast was observed between the concentrated scenario and the other two scenarios. The concentrated scenario demonstrated the greatest vulnerability to an earthquake occurring no matter the epicenter of the events.

In order to examine the impact of hydrogen demand distribution on system variables, the distribution was modified in this study. This resulted in changes to other variables that depend on the demand distribution, such as the system infrastructure. The distributed hydrogen demand scenario demonstrated greater resilience due to the indirect effects of electrolyzer distribution on generation expansion, coupled with a lower overall cost of the systems considered. While the distributed and intermediate scenarios showed no significant differences in system operation and expansion, a comparison with the concentrated scenario revealed a substantial expansion of solar infrastructure and transmission systems in the region where hydrogen demand is concentrated.

The study concluded that the distributed hydrogen topology is superior from the resilient power system planning perspective. This configuration provides a robust and less disruptive response to both electricity demand and hydrogen demand. Furthermore, it highlights the importance of the flexibility that this configuration provides in the event of seismic events.

The implications of this study for the resilient planning of electricity systems that consider hydrogen are considerable. It responds to an unexplored research space, but it is necessary. It is important to recognize that the energy transition necessitates a constant adaptation of new technologies. The integration of these technologies must be reliable and responsive to anticipated contingencies. However, it must also be resilient to respond to unavoidable natural disasters and climatic events that may become increasingly extreme if energy systems do not contribute to diversifying the matrices to respond to this problem.

6.1. Future Work

The limitations of the resilience assessment model in REMix-NZ relate to the operation of the conventional power plants of the system planned for 2050. Although these plants do not correspond to a large percentage of the installed capacity, they do not contemplate the realization of a unit commitment. Consequently, when an earthquake occurs, the simulation does not reflect the real operation of these technologies. Consequently, future work should aim to achieve a more accurate optimization of the operation of technologies that involve a longer response time when switching on and off.

This work, which was conducted with a particular focus on seismic events, employs a general approach that enables the analysis of other types of natural catastrophes that can be parameterized according to the specific hazards of the network under consideration. Consequently, it is anticipated that this study will be expanded to encompass other types of HILP events, as well as include the heat and transport energy sectors, with greater emphasis on the uncertainty surrounding such contingencies.

Bibliography

[1] O. Edenhofer, R. Pichs-Madruga, Y. Sokona, K. Seyboth, P. Matschoss, S. Kadner, T. Zwickel, P. Eickemeier, G. Hansen, S. Schlömer and C. von Stechow, "Renewable Energy Sources and Climate Change Mitigation,", Cambridge University Press., Cambridge, United Kingdom and New York, NY, USA, 2011.

[2] M. Mostafa, D. Vorwerk, J. Heise, A. Povel, N. Sanina, D. Babazadeh, C. Töbermann, A. Speerforck, C. Becker and D. Schulz, "Integrated Planning of Multi-energy Grids: Concepts and Challenges," in *Conf. on Sustainable Energy Supply and Energy Storage Systems*, Hamburg, Germany, 2022, pp. 1-7.

[3] DLR. "What is REMix?". Accessed: Apr. 12, 2024. [Online.] Available: https://dlr-ve.gitlab.io/esy/remix/framework/dev/about/introduction.html#about-introduction

[4] T. Fichter, "Long-term capacity expansion planning with variable renewable energies: enhancement of the REMix energy system modelling framework," Ph.D. dissertation, Faculty of Energy, Process Engineering and Biotechnology, University of Stuttgart, Stuttgart, DE, 2017.

[5] M. Panteli, R. Moreno, C. Martinez, A. Eduardo Alejandro and P. Mancarella, "Flexibility and Resilience in Future Low-Carbon Energy Systems," in *17th Int. Conf. on Probabilistic Modelling Applied to Power Systems*, Manchester, United Kingdom, 2022.

[6] G. Strbac, D. Kirschen and R. Moreno, "Reliability Standards for the Operation and Planning of Future Electricity Networks," *Electric Energy Systems*, vol. 1, no. 3, pp. 143-219, Dec. 2016.

[7] R. Moreno, M. Panteli, P. Mancarella, H. Rudnick, T. Lagos, A. Navarro, F. Ordonez and J. Araneda, "From Reliability to Resilience: Planning the Grid Against the Extremes," in *IEEE Power and Energy Magazine*, vol. 18, no. 4, pp. 41-53, July-Aug 2020.

[8] T. Lagos, R. Moreno, A. Navarro, M. Panteli, R. Sacaan, F. Ordonez, H. Rudnick and P. Mancarella, "Identifying Optimal Portfolios of Resilient Network Investments Against Natural Hazards, With Applications to Earthquakes," *IEEE Transactions on Power Systems*, Oct. 2019.

[9] *Hazus Earthquake Model Technical Manual,* FEMA, USA, 2020.

[10] S. Püschel-Løvengreen, S. Mhanna, P. Apablaza, P. Mancarella, J. Bukenberger and M. Ortega-Vazquez, "Assessing flexibility, risk, and resilience in low-carbon power system planning under deep uncertainty," University of Melbourne for CSIRO, Melbourne, Australia, 2023.

[11] Transpower. “Consolidated live data”. Accessed: Apr. 12, 2024. [Online.] Available: https://www.transpower.co.nz/system-operator/live-system-and-market-data/consolidated-live-data

[12] M. Gerstenberger, S. Bora, B. Bradley, C. DiCaprio, R. Van Dissen, G. Atkinson, C. Chamberlain, A. Christophersen, K. Clark, G. Coffey, C. de la Torre, S. Ellis, J. Fraser, K. Graham, J. Griffin, et al. “New Zealand National Seismic Hazard Model 2022 revision: model, hazard and process overview,” GNS, New Zealand, Rep. 57, 2022.

[13] A. Kwasinski, J. Eidinger, A. Tang, C. Tudo-Bornarel, “Performance of Electric Power Systems in the 2010–2011 Christchurch, New Zealand, Earthquake Sequence,” *Earthquake Spectra*, vol. 30, no. 1, pp. 205-230, Feb. 2014.

[14] Ministry for the Environment Manatū Mō Te Taiao, “Aotearoa New Zealand’s First Emissions Reduction Plan,” New Zealand Government, Wellington, New Zealand, 2022.

[15] Ministry of Business, Innovation and Employment Hīkina Whakatutuki, “Interim Hydrogen Roadmap,” MBIE, New Zealand, 2024.

[16] T. Khan, M. Yu and M. Waseem, “Review on recent optimization strategies for hybrid renewable energy system with hydrogen technologies: State of the art, trends and future directions,” *International Journal of Hydrogen Energy*, vol. 47, no. 60, pp. 25155-25201, Jul. 2022.

[17] R. Siddaiah and R. Saini, “A review on planning, configurations, modeling and optimization techniques of hybrid renewable energy systems for off grid applications,” *Renewable and Sustainable Energy Reviews*, vol. 58, pp. 376–396, Jan. 2016.

[18] S. Sinha and S. S. Chandel, “Review of software tools for hybrid renewable energy systems,” *Renewable and Sustainable Energy Reviews*, vol. 32, pp. 192–205, Apr. 2014.

[19] S. Peláez-Peláez, A. Colmenar-Santos, C. Pérez-Molina, A. Rosales and E. Rosales-Asensio, “Techno-economic analysis of a heat and power combination system based on hybrid photovoltaic-fuel cell systems using hydrogen as an energy vector,” *Energy*, vol. 224, p. 120110, Feb. 2021.

[20] T. Salameh, M. Ali Abdelkareem, A. Olabi, E. Taha Sayed, M. Al-Chaderchi and H. Rezk, “Integrated standalone hybrid solar PV, fuel cell and diesel generator power system for battery or supercapacitor storage systems in Khorfakkan, United Arab Emirates,” *International Journal of Hydrogen Energy*, vol. 46, no. 8, pp. 6014-6027, Jan. 2021.

[21] M. Saif, D. Zhang, L. Wang, M. Mohan, M. Panjwani, C. Li, Y. Zhang and M. Li, “Efficient photovoltaics-integrated hydrogen fuel cell-based hybrid system: Energy management and optimal configuration,” *Journal of Renewable and Sustainable Energy*, vol. 13, no. 1, pp. 013502, Jan. 2021.

[22] M. S. Behzadi and M. Niasati, “Comparative performance analysis of a hybrid PV/FC/battery stand-alone system using different power management strategies and sizing approaches,” *International Journal of Hydrogen Energy*, vol. 40, no. 1, pp. 538-548, Jan. 2015.

[23] T. Tezer, R. Yaman and G. Yaman, “Evaluation of approaches used for optimization

of stand-alone hybrid renewable energy systems," *Renewable and Sustainable Energy Reviews*, vol. 73, pp. 840-853, Jun. 2017.
Renewable and Sustainable Energy Reviews, vol. 135, pp. 1412–1434, May. 2019.

[24] A. Naderipour, Z. Abdul-Malek, S. Arabi, H. Kamyab, A. Reza, S. Shahrokhi and J. Jaromír, "Comparative evaluation of hybrid photovoltaic, wind, tidal and fuel cell clean system design for different regions with remote application considering cost," *Journal of Clean Production*, vol. 283, p. 124207, Feb. 2021.

[25] M. Amer, A. Namaane and N.K. M'Sirdi, "Optimization of Hybrid Renewable Energy Systems (HRES) Using PSO for Cost Reduction," *Energy Procedia*, vol. 42, pp. 318-327, 2013.

[26] M. Waseem, Z. Lin, S. Liu, Z. Zhang, T. Aziz and D. Khan, "Fuzzy compromised solution-based novel home appliances scheduling and demand response with optimal dispatch of distributed energy resources," *Applied Energy*, vol. 290, p. 116761, May. 2021.

[27] W. Zhang, A. Maleki, M. A. Rosen, and J. Liu, "Optimization with a simulated annealing algorithm of a hybrid system for renewable energy including battery and hydrogen storage," *Energy*, vol. 163, pp. 191–207, Nov. 2018.

[28] A. Ibáñez-Rioja, P. Puranem, L. Järvinen, A. Kosonen, V. Ruuskanen, J. Ahola and J. Koponen, "Simulation methodology for an off-grid solar–battery–water electrolyzer plant: Simultaneous optimization of component capacities and system control," *Applied Energy*, vol. 307, p. 118157, Feb. 2022.

[29] H. Tebibel, "Methodology for multi-objective optimization of wind turbine/battery/electrolyzer system for decentralized clean hydrogen production using an adapted power management strategy for low wind speed conditions," *Energy Conversion and Management*, vol. 238, p. 114125, Jun. 2021.

[30] I. A. Ibrahim, T. Khatib and A. Mohamed, "Optimal sizing of a standalone photovoltaic system for remote housing electrification using numerical algorithm and improved system models," *Energy*, vol. 126, pp. 392-403, May. 2017.

[31] A. Y. Hatata, G. Osman, and M. M. Aladl, "An optimization method for sizing a solar/wind/battery hybrid power system based on the artificial immune system," *Sustainable Energy Technologies and Assessments*, vol. 27, pp. 83–93, Jun. 2018.

[32] S. Upadhyay and M.P. Sharma, "A review on configurations, control and sizing methodologies of hybrid energy systems," *Renewable and Sustainable Energy Reviews*, vol. 38, pp. 47-63, Oct. 2014.

[33] S. Sanajaoba and E. Fernandez, "Maiden application of Cuckoo Search algorithm for optimal sizing of a remote hybrid renewable energy System," *Renewable Energy*, vol. 96, pp. 1–10, Oct. 2016.

[34] A. Chauhan and R.P. Saini, "A review on Integrated Renewable Energy System based power generation for stand-alone applications: Configurations, storage options, sizing methodologies and control," *Renewable and Sustainable Energy Reviews*, vol. 38, pp. 99-120, Oct. 2014.

[35] M. Haddad, J. M. Nicod, C. Varnier, and M.-C. Péra, "Mixed Integer Linear Programming Approach to Optimize the Hybrid Renewable Energy System Management

for supplying a Stand-Alone Data Center; Mixed Integer Linear Programming Approach to Optimize the Hybrid Renewable Energy System Management for supplying a Stand-Alone Data Center," in *10th Int. Green and Sustainable Computing Conf.*, Alexandria, VA, USA, 2019.

[36] D. Cho and J. Valenzuela, "A scenario-based optimization model for determining the capacity of a residential off-grid PV-battery system," *Solar Energy*, vol. 233, pp. 478–488, Feb. 2022.

[37] A. de Corato, I. Saedi, S. Riaz, and P. Mancarella, "Aggregated flexibility from multiple power-to-gas units in integrated electricity-gas-hydrogen distribution systems," *Electric Power Systems Research*, vol. 212, p. 108409, Nov. 2022.

[38] S. Basnet, K. Deschinkel, L. Le Moyne and M-C Péra. "A review on recent standalone and grid integrated hybrid renewable energy systems: System optimization and energy management strategies," *Renewable Energy Focus*, vol. 46, pp. 103-125, Sept. 2023.

[39] PyPSA. *Introduction*. Accessed: Apr. 12, 2024. [Online.] Available: https://pypsa.readthedocs.io/en/latest/introduction.html

[40] FINE. *ETHOS.FINE - Framework for Integrated Energy System Assessment*. Accessed: Apr. 12, 2024. [Online.] Available: https://vsa-fine.readthedocs.io/en/latest/

[41] PyPSA. *Contingency Analysis*. Accessed: Apr. 12, 2024. [Online.] Available: https://pypsa.readthedocs.io/en/latest/contingency_analysis.html

[42] H. C. Gils, Y. Scholz, T. Pregger, D. L. de Tena and D. Heide, "Integrated modelling of variable renewable energy-based power supply in Europe," *Energy*, vol. 123, pp. 173-188, Mar. 2017.

[43] CPLEX. . Accessed: Aug. 31, 2024. [Online.] Available: https://www.ibm.com/es-es/products/ilog-cplex-optimization-studio

[44] GUROBI. *Gurobi Optimization*. Accessed: Aug. 31, 2024. [Online.] Available: https://www.gurobi.com/

[45] H. C. Gils, H. Gardian and J. Schmugge, "Interaction of hydrogen infrastructures with other sector coupling options towards a zero-emission energy system in Germany," *Renewable Energy*, vol. 180, pp. 140-156, Dec. 2021.

[46] M. Panteli and P. Mancarella, "Influence of extreme weather and climate change on the resilience of power systems: Impacts and possible mitigation strategies," *Electric Power Systems Research*, vol. 127, pp. 259–270, Oct. 2015.

[47] M. Bruneau, S. Chang, R. Eguchi, G. Lee, T. O'Rourke, A. Reinhorn, M. Shinozuka, K. Tierney, W. Wallace and D. Winterfeldt, "A Framework to Quantitatively Assess and Enhance the Seismic Resilience of Communities," in *13th World Conf. on Earthquake Engineering*, Vancouver, B.C., Canada, 2004.

[48] E. Ciapessoni, D. Cirio, A. Pitto, M. Van Harte and M. Panteli. "Power System Resilience: definition, features and properties," CIGRE, CSE030, 2023.

[49] M. Panteli, D. N. Trakas, P. Mancarella and N. D. Hatziargyriou, "Power Systems Resilience Assessment: Hardening and Smart Operational Enhancement Strategies," *Proceedings of the IEEE*, vol. 105, no. 7, pp. 1202-1213, Jul. 2017.

[50] B. Ayyub, (2013). "Systems resilience for multihazard environments: Definition, me-

trics, and valuation for decision making," *Risk Analysis*, vol. 34, no. 2, Feb. 2014.

[51] A. Decò, P. Bocchini and D.M. Frangopol. (2013). "A probabilistic approach for the prediction of seismic resilience of bridges," *Earthquake Engineering & Structural Dynamics*, vol. 42 no. 10, pp. 1469–1487. Ago. 2013.

[52] C. Nan and G. Sansavini, "A quantitative method for assessing resilience of interdependent infrastructures," *Reliability Engineering & System Safetydoi*, vol. 157, pp. 35–53, Jan. 2017.

[53] P. Gasser, P. Lustenberger, M. Cinelli, W. Kim, M. Spada, B. Matteo, H. Peter, S. Stefan and Su. Bozidar and Tianyin, "A review on resilience assessment of energy systems," *Sustainable and Resilient Infrastructure* vol. 6, pp. 1-27, Jun. 2019.

[54] H. Raoufi, V. Vahidinasab and K. Mehran, "Power Systems Resilience Metrics: A Comprehensive Review of Challenges and Outlook," *Sustainability*, vol. 12, no. 22, p. 9698, Nov. 2020.

[55] H.R. Sayarshad, O. Sabarshad and N. Amjady, "Evaluating resiliency of electric power generators against earthquake to maintain synchronism," *Electric Power Systems Research*, vol. 210, p. 108127, Sept. 2022.

[56] N. Bhusal, M. Abdelmalak, M. Kamruzzaman and M. Benidris, "Power System Resilience: Current Practices, Challenges, and Future Directions," *IEEE Access*, vol. 8, Jan. 2020.

[57] A. Schweikert, L. Nield, E. Otto and M. Dienert, *Resilience and Critical Power System Infrastructure,* World Bank Group, Colorado, USA, 2019.

[58] S. Dahal and N.R. Karki. "Transmission Systems Resilience Assessment: A Case Study in Integrated Nepal Power System," in *10th IOE Graduate Conf.*, Pokhara, Nepal, 2021.

[59] Y. Yang, W. Tang, Y. Liu, Y. Xin, and Q. Wu, "Quantitative Resilience Assessment for Power Transmission Systems Under Typhoon Weather," *IEEE Access*, vol. 6, pp. 40747-40756, Jul. 2018.

[60] R. Miller, "Resilience assessment of active distribution networks," Ph.D. dissertation, Norm Asbjornson College of Engineering, Montana State University-Bozeman, Montana, USA, 2021.

[61] H. Hou, J. Tang, Z. Zhang, Z. Wang, R. Wei, L. Wang, H. He and X. Wu, "Resilience enhancement of distribution network under typhoon disaster based on two-stage stochastic programming," *Applied Energy*, vol. 338, p. 120892, May. 2023.

[62] S. Espinoza, M. Panteli, P. Mancarella, and H. Rudnick, "Multi-phase assessment and adaptation of power systems resilience to natural hazards," *Electric Power Systems Research*, vol. 136, pp. 352–361, Jul. 2016.

[63] O.J. Ayamolowo, P. Manditereza and K. Kusakana, "Combined Generation and Transmission Expansion Planning Model for Improved Modern Power System Resilience," *Electric Power Components and Systems*, vol. 51, no. 9, pp. 898–914, Feb. 2023.

[64] D. Byles, P. Kuretich and S. Mohagheghi, "Generation and Transmission Expansion Planning: Nexus of Resilience, Sustainability, and Equity" *Processes*, vol. 12, no. 3,

p. 590, Mar. 2024.

[65] B. Cheng, L. Nozick and I. Dobson, “Investment planning for earthquake-resilient electric power systems considering cascading outages,” *Earthquake Spectra*, vol. 38, no. 3, pp. 1734-1760, Feb. 2022.

[66] J. Barrera, P. Beaupuits, E. Moreno, R. Moreno and F. D. Muñoz, “Planning resilient networks against natural hazards: Understanding the importance of correlated failures and the value of flexible transmission assets,” *Electric Power Systems Research*, vol. 197, pp. 107280, Aug. 2021.

[67] A. Villamarín-Jácome and R. Moreno, “Seismic Resilience Assessment of Electric Power Systems Using a Substation Bay-level Model,” in *17th Int. Conf. on Probabilistic Methods Applied to Power Systems*, Manchester, United Kingdom, 2022, pp. 1-6.

[68] W. Shi, H. Liang and M. Bittner, “Stochastic Planning for Power Distribution System Resilience Enhancement Against Earthquakes Considering Mobile Energy Resources,” *IEEE Transactions on Sustainable Energy*, vol. 15, no. 1, pp. 414-428, Jan. 2024.

[69] R. Saberi, H. Falaghi, M. Esmaeeli, M. Ramezani, A. Ashoornezhad and R. Izadpanah, “Power distribution network expansion planning to improve resilience,” *IET Generation, Transmission & Distribution*, vol. 17, pp. 4701–4716, Jan. 2023.

[70] M. Nazemi, M. Moeini-Aghtaie, M. Fotuhi-Firuzabad and P. Dehghanian, “Energy Storage Planning for Enhanced Resilience of Power Distribution Networks Against Earthquakes,” *IEEE Transactions on Sustainable Energy*, vol. 11, no. 2, pp. 1-1, Mar. 2019.

[71] R. Sacaan, H. Rudnick, T. Lagos, F. Ordóñez, A. Navarro-Espinosa and R. Moreno, “Improving power system reliability through optimization via simulation,” in *2017 IEEE Manchester PowerTech*, Manchester, UK, 2017, pp. 1-6.

[72] M. Saltos-Rodríguez, M. Aguirre-Velasco, A. Velásquez-Lozano, A. Villamarín-Jácome, J. R. Haro and D. Ortiz-Villalba, “Resilience Assessment in Electric Power Systems Against Volcanic Eruptions: Case on Lahars Occurrence,” in *2021 IEEE Green Technologies Conference*, Denver, CO, USA, 2021, pp. 305-311.

[73] H. Liu, C. Wang, P. Ju and H. Li, “A sequentially preventive model enhancing power system resilience against extreme-weather-triggered failures,” *Renewable and Sustainable Energy Reviews*. vol. 156, p. 111945, Mar. 2022.

[74] A. Poudyal, S. Lamichhane, A. Dubey and J.C. Prado, “Resilience-driven Planning of Electric Power Systems Against Extreme Weather Events,” Nov. 2023.

[75] S. Espinoza, A. Poulos, H. Rudnick, J.C. de la Llera, M. Panteli and P. Mancarella, “Risk and resilience assessment with component criticality ranking of electric power systems subject to earthquakes,” *IEEE Systems Journal*, vol. 14 no. 2, pp. 2837–2848, Jun. 2020.

[76] B. Johnson, V. Chalishazar, E. Cotilla-Sanchez and T.K. Brekken. “A Monte Carlo methodology for earthquake impact analysis on the electrical grid,” *Electric Power Systems Research*, vol. 184, p. 106332, Jul. 2020.

[77] V. Chalishazar, C. Huo, I. Fox, T. Hagan, E. Cotilla-Sanchez, A. Von Jouanne, J, Zhang, T. Brekken and R.B, Bass. “Modeling power system buses using performan-

ce based earthquake engineering methods," in *2017 IEEE Power & Energy Society General Meeting*, Chicago, IL, USA, Jul. 2017, pp. 1–5.

[78] M. Panteli, P. Mancarella, D. N. Trakas, E. Kyriakides and N. D. Hatziargyriou, "Metrics and Quantification of Operational and Infrastructure Resilience in Power Systems," *IEEE Transactions on Power Systems*, vol. 32, no. 6, pp. 4732-4742, Nov. 2017.

[79] A.R. Jordehi, S.A. Mansouri, M. Tostado-Véliz, A. Iqbal, M. Marzband and F. Jurado, "Industrial energy hubs with electric, thermal and hydrogen demands for resilience enhancement of mobile storage-integrated power systems," *International Journal of Hydrogen Energy*, vol. 50, pp. 77-91, Jan. 2024.

[80] A. Cardenas, "An operational resilience objective to integrate in capacity expansion models for green hydrogen production through HRES," MSc dissertation, Department of Electrical Engineering, University of Chile, Santiago, CL, 2023.

[81] H. Haggi, W. Sun, J.M. Fenton and P. Brooker, "Proactive Scheduling of Hydrogen Systems for Resilience Enhancement of Distribution Networks," in *2021 IEEE Kansas Power and Energy Conference*, Manhattan, KS, USA, 2021, pp. 1-5.

[82] T. Meares, H. Tyrell and R. Pendlebury, *Hydrogen: the role of the hydrogen production industry in providing system services to the NEM,* AEMC, Sydney, Australia, 2022.

[83] S. Sasanpour, K-K Cao, H.C. Gils and P. Jochem, "Strategic policy targets and the contribution of hydrogen in a 100 % renewable European power system," *Energy Reports*, vol. 7, pp. 4595-4608, Nov. 2021.

[84] F.A. Plazas-Niño, R. Yeganyan, C. Cannone, M. Howells, B. Borba and J. Quirós-Tortós, "Open energy system modelling for low-emission hydrogen roadmap planning: The case of Colombia," *Energy Strategy Reviews*, vol. 53, p. 101401, May. 2024.

[85] A. Constantin, "Nuclear hydrogen projects to support clean energy transition: Updates on international initiatives and IAEA activities," *International Journal of Hydrogen Energy*, vol. 54, pp. 768-779, Feb. 2024.

[86] C. Park, M.Koo, J. Woo, B. Il Hong and J. Shin, "Economic valuation of green hydrogen charging compared to gray hydrogen charging: The case of South Korea," *International Journal of Hydrogen Energy*, vol. 47, no. 32, pp. 14393-14403, Apr. 2022.

[87] Y. Dong, Z. Han, C. Li, S. Ma and Z. Ma, "Research on the optimal planning method of hydrogen-storage units in wind–hydrogen energy system considering hydrogen energy source," *Energy Reports*, vol. 9, pp. 1258-1264, Oct. 2023.

[88] B. Modu, M.P. Abdullah, A.L. Bukar, M.F. Hamza and M.S. Adewolu, "Energy management and capacity planning of photovoltaic-wind-biomass energy system considering hydrogen-battery storage," *Journal of Energy Storage*, vol. 73, p. 109294, Dec. 2023.

[89] Z. Li, Y. Xia, Y. Bo and W. Wei, "Optimal planning for electricity-hydrogen integrated energy system considering multiple timescale operations and representative time-period selection," *Applied Energy*, vol. 362, p. 122965, May. 2024.

[90] National Emergency Management Agency. *Learn About Hazards*. Accessed: May 2, 2024. [Online.] Available: https://www.civildefence.govt.nz/get-ready/learn-about

-hazards

[91] Environmental Health Intelligence New Zealand. *About natural hazards: New Zealand Environment Health Indicators*. Accessed: May 2, 2024. [Online.] Available: https://www.ehinz.ac.nz/indicators/population-vulnerability/about-natural-hazards/

[92] OECD and The World Bank. "Fiscal Resilience to Natural Disasters: Lessons from Country Experiences," OECD Publishing, Paris, France, 2019.

[93] Climate Change Knowledge Portal. *New Zealand Vulnerability*. Accessed: May 3, 2024. [Online.] Available: https://climateknowledgeportal.worldbank.org/country/new-zealand/vulnerability

[94] Natural Hazards Commission Toka Tü Ake. *Natural Hazards where you Live*. Accessed: May 3, 2024. [Online.] Available: https://www.eqc.govt.nz/be-prepared/natural-hazards-where-you-live/

[95] GeoNet. *Earthquakes - M 7.2 Darfield (Canterbury) Sat, Sep 4 2010*. Accessed: May 4, 2024. [Online.] Available: https://www.geonet.org.nz/earthquake/story/3366146

[96] WorldData. *Earthquakes in New Zealand*. Accessed: May 5, 2024. [Online.] Available: https://www.worlddata.info/oceania/new-zealand/earthquakes.php

[97] Ministry of Business, Innovation and Employment Hīkina Whakatutuki, "Energy In New Zealand 23," MBIE, Wellington, New Zealand, 2023.

[98] New Zealand Parliamentary Counsel Office/Te Tari Tohutohu Pāremata, *Climate Change Response (Zero Carbon) Amendment Act 2019*, New Zealand Government, New Zealand, 2019.

[99] Ministry for the Environment Manatū Mō Te Taiao. *Climate Change Response (Zero Carbon) Amendment Act 2019*. Accessed: May 9, 2024. [Online.] Available: https://environment.govt.nz/acts-and-regulations/acts/climate-change-response-amendment-act-2019/

[100] Ministry of Business, Innovation and Employment Hīkina Whakatutuki, *Terms of Reference - New Zealand Energy Strategy,* MBIE, New Zealand, 2022.

[101] Ministry of Business, Innovation and Employment Hīkina Whakatutuki, *New Zealand's Hydrogen Regulatory Pathway,* MBIE, New Zealand, 2022.

[102] M. Manjunath, H.C. Gils, M. Yeligeti, M. Fyta, J. Haas and W. Nowak,"Monitoring resilience of future energy systems," MSc Dissertation, Faculty of Energy, Process Engineering and Biotechnology, University of Stuttgart, Stuttgart, DE, 2020.

[103] C. B. Crouse, "Crouse Ground-Motion Attenuation Equations for Earthquakes on the Cascadia Subduction Zone," *Earthquake Spectra*, vol. 7, no. 2, pp. 201-236, May. 1991.

[104] S. R. Uma, V. Sadashiva, S. L. Lin and M. Nayyerloo, "Fragility Curves for New Zealand Buildings With Reflections from the Canterbury Earthquake Sequence," in *16th World Conference on Earthquake*, Santiago, Chile, 2017, 309.

[105] I. Kongar, S. Giovinazzi and T. Rossetto, "Seismic performance of buried electrical cables: evidence-based repair rates and fragility functions," *Bulletin of Earthquake Engineering*, vol. 15, pp. 3151-3181, Dec. 2016.

[106] H. Vatankhah Ghadim, R. A. M. Peer, E.G. Read and J. Haas, "How much hydrogen

could we need in New Zealand? Understanding the diverse hydrogen applications and their regional mapping," *Journal of the Royal Society of New Zealand*, pp. 1–20, Mar. 2024.

Annexes

Annex A. Installed capacities for New Zealand 2050

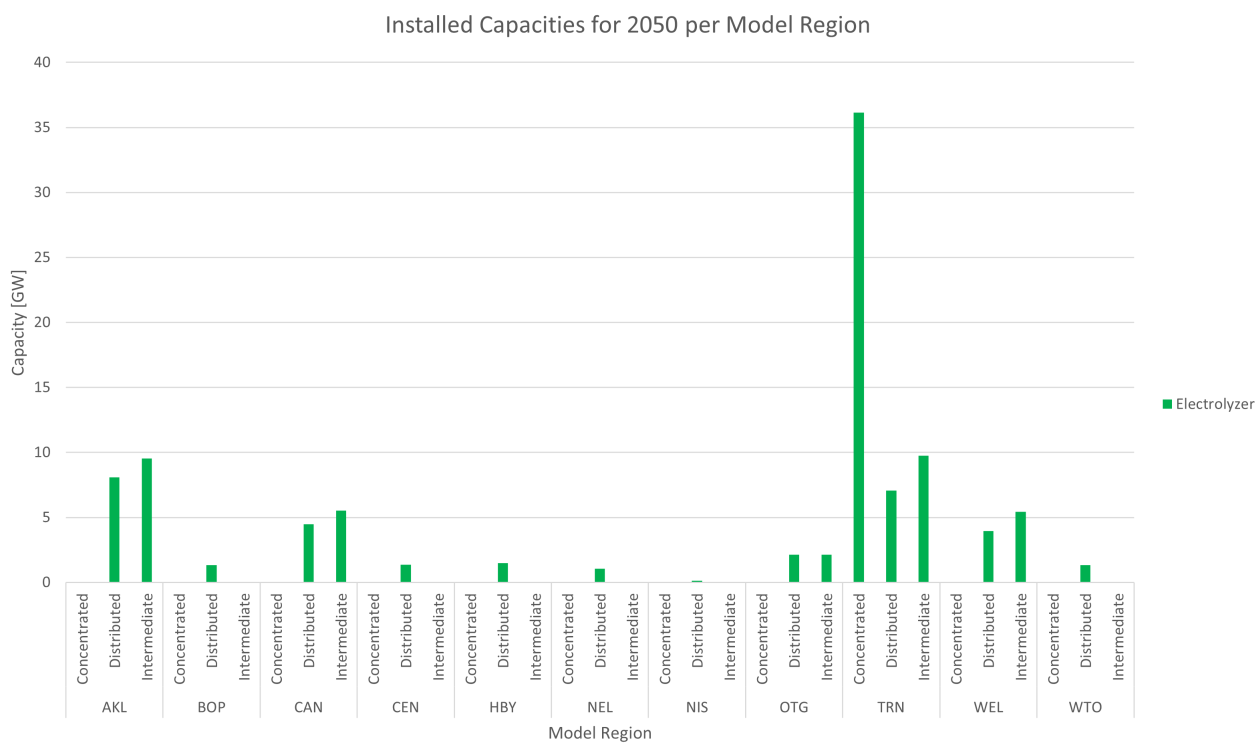

Figura A.1: Installed capacities of electrolyzers in each hydrogen scenario for the year 2050 according to the New Zealand model region.

A.1. Case Study: Concentrated H2 Demand 2050

Table A.1: Installed generation capacities obtained when planning the "Concentrated H2 Demand" Scenario.

Year	Technology	Capacity [GW]
2050	pv_central_fixed	335
2050	Battery	178
2050	pv_central_track_azimuth	51
2050	wind_onshore	33
2050	OCGT	8.9
2050	Hydro	6.0
2050	CCGT	5.9
2050	geoth	1.0
2050	GT	0.8
2050	DIE	0.2
2050	COAL	0.1
2050	BIO	0.0
2050	pv_decentral	0.0
2050	Total	622

Table A.2: Installed hydrogen generation capacities obtained when planning the "Concentrated H2 Demand" Scenario.

Year	Technology	Capacity [GW]
2050	Electrolyzer	36

A.2. Case Study: Intermediate H2 Demand 2050

Table A.3: Installed generation capacities obtained when planning the "Intermediate H2 Demand" Scenario.

Year	Technology	Capacity [GW]
2050	pv_central_fixed	359
2050	Battery	166
2050	wind_onshore	29
2050	Hydro	6.0
2050	OCGT	5.3
2050	CCGT	5.2
2050	geoth	1.0
2050	wind_offshore_floating	0.9
2050	GT	0.8
2050	DIE	0.2
2050	pv_central_track_azimuth	0.2
2050	COAL	0.1
2050	BIO	0.0
2050	pv_decentral	0.0
2050	Total	574

Table A.4: Installed hydrogen generation capacities obtained when planning the "Intermediate H2 Demand" Scenario.

Year	Technology	Capacity [GW]
2050	Electrolyzer	32

A.3. Case Study: Distributed H2 Demand in 2050

Table A.5: Installed generation capacities obtained when planning the "Distributed H2 Demand" Scenario.

Year	Technology	Capacity [GW]
2050	pv_central_fixed	356
2050	Battery	170
2050	wind_onshore	30
2050	OCGT	6.1
2050	Hydro	6.0
2050	pv_central_track_azimuth	5.1
2050	CCGT	4.9
2050	geoth	1.0
2050	GT	0.8
2050	DIE	0.2
2050	wind_offshore_floating	0.1
2050	COAL	0.1
2050	BIO	0.0
2050	pv_decentral	0.0
2050	Total	582

Table A.6: Installed hydrogen generation capacities obtained when planning the "Distributed H2 Demand" Scenario.

Year	Technology	Capacity [GW]
2050	Electrolyzer	32

Annex B. Investment Cost for New Zealand 2050 per Model Region

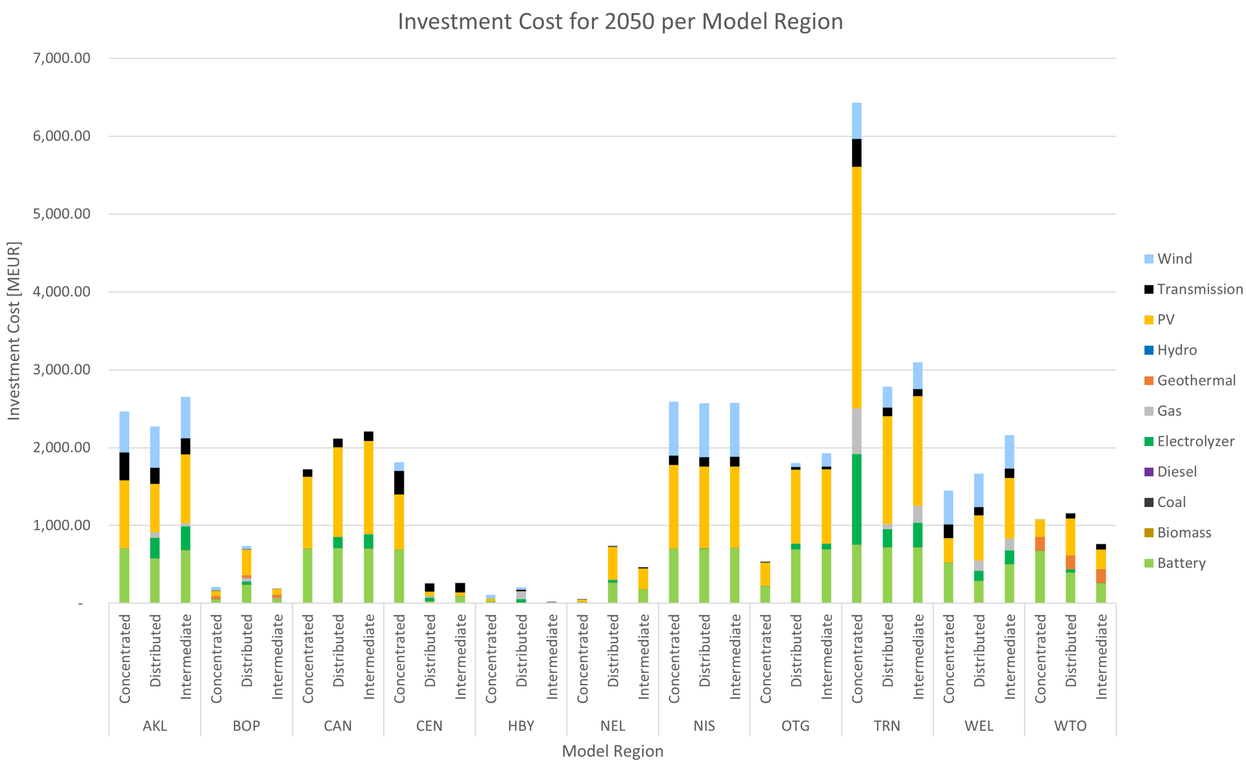

Figura B.1: Investment cost per model region in each hydrogen scenario for the year 2050 according to the New Zealand model region.